J. Indian Inst. Sci., Jan.–Feb. 1996, 75, 15–35.

Wear and seizure of aluminium–silicon-based IC engine component materials

S. K. BISWAS AND A. SOMI REDDY
Department of Mechanical Engineering, Indian Institute of Science, Bangalore 560 012.

Received on November 5, 1995.

Abstract

Aluminium–silicon-based alloys are important materials for internal combustion engines. Experimental work done in this area over the last 15 years in the authors' laboratory is reported and forms the basis for qualitative models for the wear and seizure of alloys. Such models are useful for selection and/or design of materials for IC engines of the future.

Keywords: Wear, IC engines, engine materials, aluminium alloys.

1. Introduction

1.1. *Wear and scuffing of engine components*

Wear, scuffing and seizure are problems of internal combustion (IC) engine components. In internal combustion engines the wear resistance and short-term engine efficiency and performance are in some sense antagonistic. For high performance and efficiency it is desirable to conserve heat in the chamber by using low conductivity materials. High efficiency is also promoted by clearances between ring and liner and good fits of the ring in the piston. The consequent high temperature reduces the mechanical strengths of components aiding the cause of wear. Small clearances readily allow puncturing of the hydrodynamic film and frequent metal-to-metal contact. This clearly increases the occurrence of events which generate wear debris. The high temperature and low clearance eventually cause seizure through plastic deformation and adhesion.

Engine materials are rarely chosen for wear resistance, but are selected for promoting engine performance. If the ensuing wear and scuffing are very poor some changes, such as alloying additions and heat treatment, are sought to provide marginal improvement in high-temperature strength and consequent wear and scuffing resistance without any significant sacrifice to the performance. This short-term philosophy is indeed erroneous as it may lead to rapid deterioration of performance within short time and lead to catastrophic failures. A more balanced sub-optimal approach is clearly indicated for the future.

Traditionally, cylinder liners are made of grey cast iron (CI), which is heavy and has a low power-to-weight ratio. The wear and scuffing resistance can be improved by the

addition of alloying elements, surface treatment such as nitriding and other treatments which control the graphite size. Graphite optimally sized and spaced is a solid lubricant which augments wear and scuff resistance. Steel suitably alloyed and surface treated (nitriding, nitrosulphiding, chrome plating) is a good candidate for a liner due to its workability and drawability.

Aluminium-based alloys are clearly attractive alternatives to iron-based ones as they provide high power-to-weight ratios (10–12). Aluminium alloys are very popular piston alloys. Low density and high conductivity provide these alloys with excellent credentials for high-performance engines. Low density leads to lower inertia forces and low wear. The high thermal conductivity allows the skirts to carry strong oil films. This creates favourable anti-friction condition at the cylinder face.

The high coefficient of thermal expansion, compared to grey CI pistons, can be reduced substantially by increasing the silicon content in the hypereutectic range. This addition increases the scuffing resistance but reduces strength. Additions of Cu, Mg and Ni also improve the scuffing resistance. There is a lack of unanimity among piston manufacturers about the optimum silicon content. Manufacturers in US and Europe use 5 to 30% Si. A low-silicon alloy has high ductility and low strength. The strength increases with silicon content up to the eutectic and then decreases while the fatigue strength decreases with increasing silicon content. The coefficient of expansion and thermal conductivity decreases with increasing silicon content.

The traditional material for piston rings is grey CI. It has generally been found to give satisfactory performance in low- and medium-rated engines. Unfortunately it has poor fatigue strength. Malleable and nodular iron has higher fatigue strength but has poor wear resistance. Rings made from this iron and used in heavy-duty engines are chrome plated to enhance longevity.

Piston rings made out of steel have also been used in engines where the working temperatures and working loads are high. Fatigue strength and elastic modulus of steel are significantly better than those of CI and are easy to make. The scuffing and wear resistance of steel in the unhardened condition is however not very satisfactory. Surface hardening treatments such as nitriding and chromium plating are used to overcome these constraints.

1.2. *The problem formulation*

The above discussion points to the wealth of experience and information about engine materials which has accumulated in the industry over the years. In terms of engine performance aluminium-based cylinder blocks and pistons with steel rings now challenge the traditional iron-based combinations. While this combination may be ideal for the future, any serious effort towards optimal material selection/processing or design of new materials for specific and futuristic applications is seriously hampered as knowledge in this area has a highly empirical flavour. We have little understanding of processes which lead to wear and scuffing/seizure of complex material combinations over a wide range of operating conditions.

Through analytical models of the IC engine wear/seizure problem taken up from the late 70s and early 80s, our understanding of the problem is now better. More importantly, the basic knowledge accumulated on the wear and seizure of metal components provides a basis for the design of MMCs or ceramic-based engine components.

The focus of this paper is on the tribological interaction of aluminium–silicon-based alloys with steel. Such a study, to be useful for IC engine materials design and selection

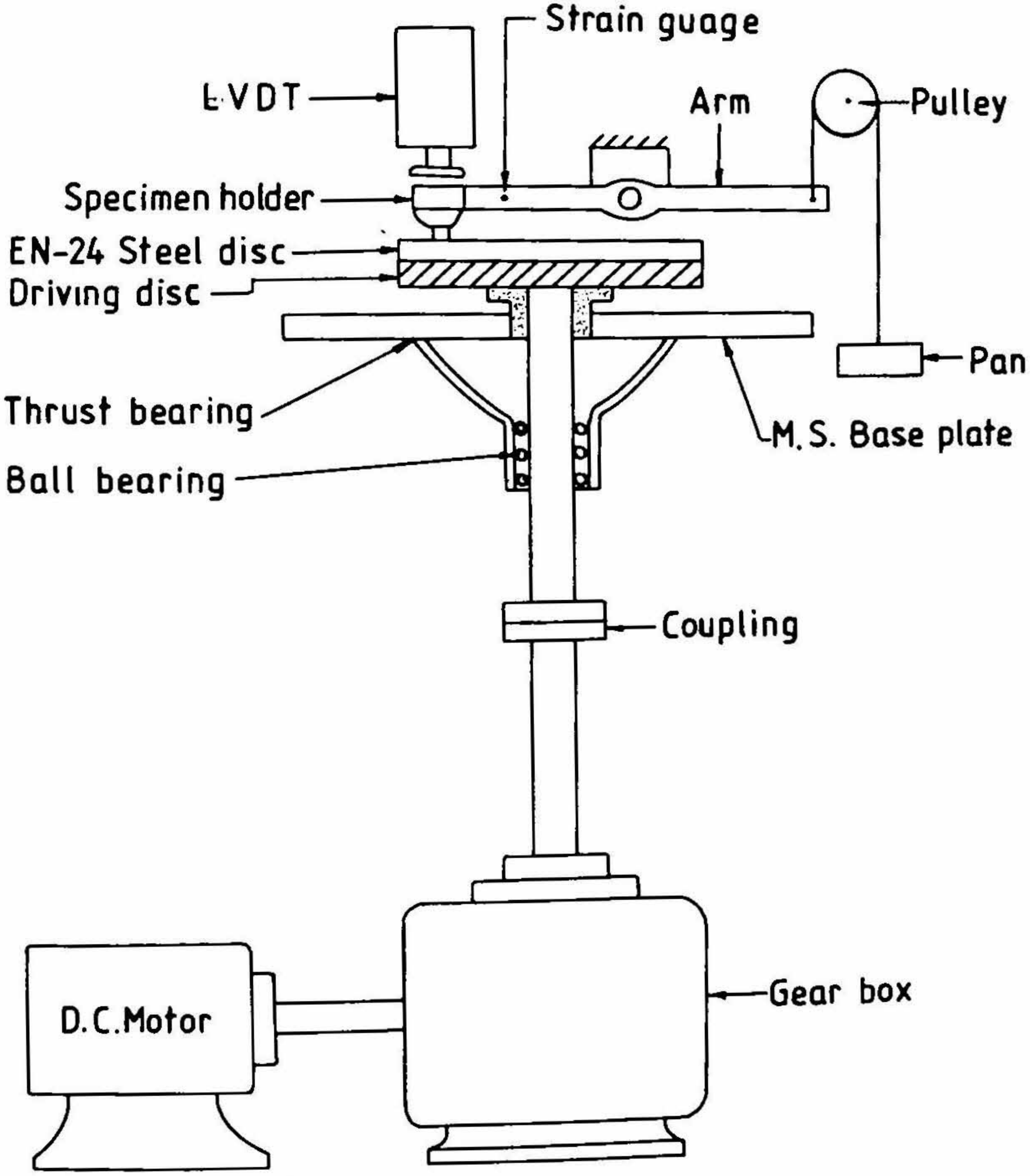

FIG. 1a. Schematic diagram of the pin-on-disc machine.

ought to be carried out in reciprocation in an atmosphere of corrosive gases typical of the engine and under pressure and speed. Clearly an attempt at studying a very complex interaction without understanding the more elementary ones can lead to confusion and be unproductive.

The problem is thus studied initially in unidirectional sliding under nominally dry conditions and under pressure. Speed conditions generate both mild and severe wear but no seizure. The materials under focus, initially in consonance, are binary (aluminium and silicon) alloys. Complexities were introduced into the tests in a step-by-step manner; a) the alloys were made more complex by additions and heat treatment; b) the interaction was made more complex by introducing reciprocation, and c) the speed and load ranges were extended to include scuffing and seizure. The chemical and erosive aspects of the engine wear problem have still not received enough attention. The present work addresses the following broad issues.

1. Classification of wear
2. Effect of silicon and alloying elements on wear and seizure
3. Mechanism of wear
4. Mechanism of seizure.

2. Experimental details

2.1. *Test equipment*

The three principal tribometers used in the work reported here are shown in Figs 1 and 2.

1. Pin-on-disc machine (Fig.1a): A pin machined from the test material is loaded normally against the flat surface of a ground EN24 disc (55RC). The disc is rotated and the friction force recorded using a load cell and wear estimated from the vertical displacement of the pin measured using an LVDT.

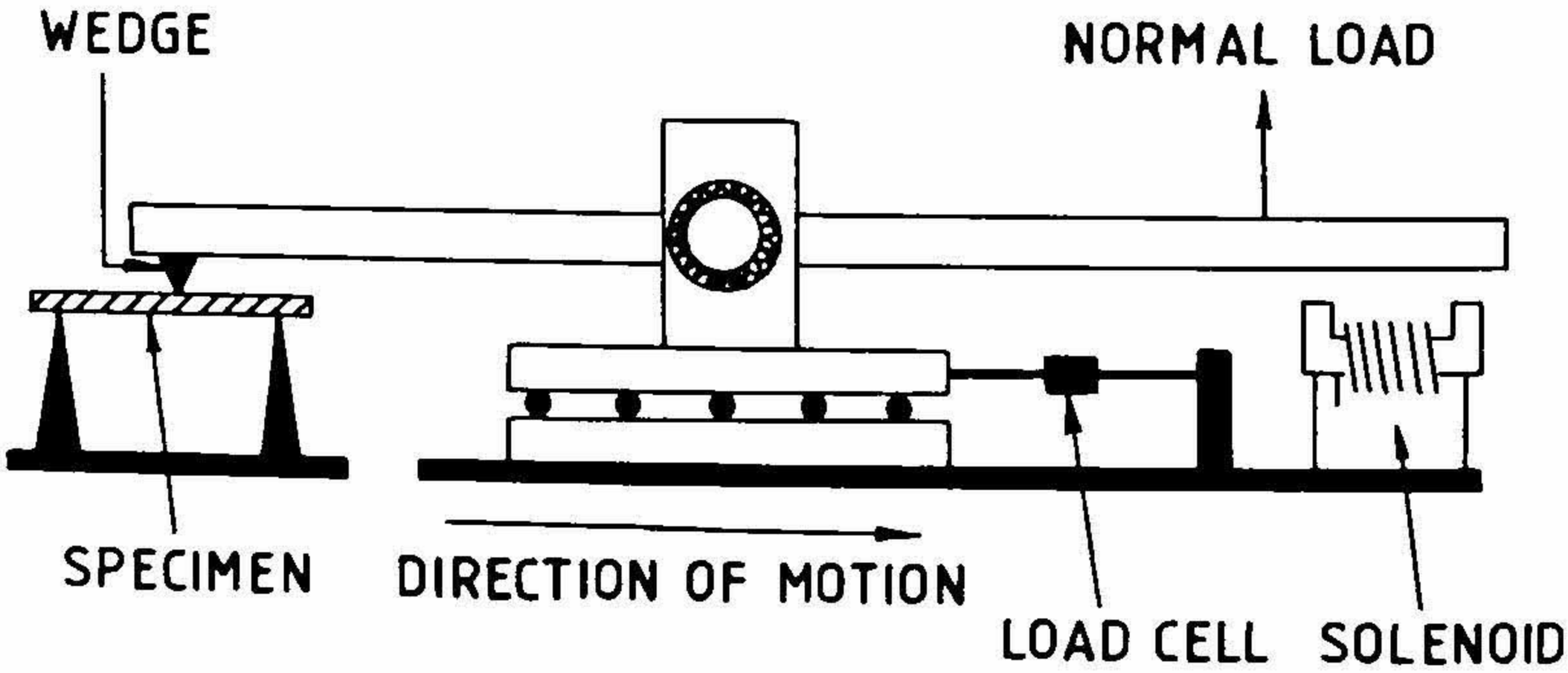

FIG. 1b. Schematic diagram of the scribing machine.

2. Scribing-a-scratch machine (Fig. 1b): An SiC wedge bearing upon the test flat is dragged by a motor. The friction force is measured by using a flexure mounted on the wedge support. A provision is built (not shown) into the equipment to conduct the scribing experiments under isothermal conditions at different temperatures. The specimen mount in this case is put inside a small muffle furnace[1] .

3. Reciprocating rig (Fig. 2): Normally loaded test pins are slid against EN24 steel flats.The flats reciprocate in a horizontal plane. The friction load and pin displacement are measured using a load cell and an LVDT, respectively. The signal from the load cell is recorded after passing through a low-pass filter[2].

2.2. *Test procedure*

Most sliding (unidirectional and reciprocating) experiments were done in a continuous loading mode. Of the two principal experimental variables—load and sliding speed—one is kept constant while the other is varied in steps over a test range. When the variable is changed the new wear is allowed to reach a steady state before the variable level is changed again.

Some experiments were also done at one combination of speed and load over a long period of time.

2.3. *Test materials*

Unmodified aluminium–silicon alloys were melted in graphite crucibles and cast into 20-mm diameter finger moulds before degassing. Copper, magnesium and nickel were added to the melt. Binary and multi-component alloys in as-cast and heat-treated conditions were tested. The compositional range was:

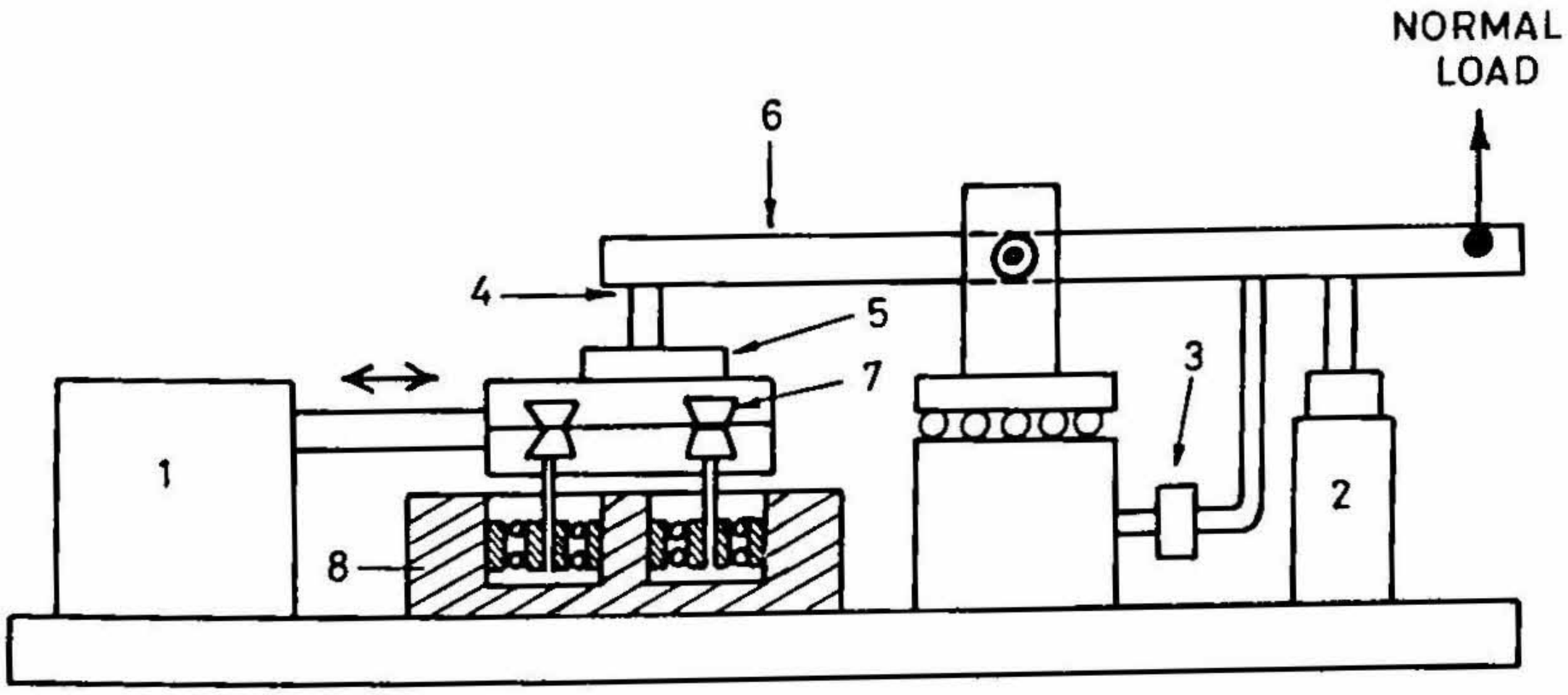

1. Motor and crank arrangement, 2. Linear variable differential transducer (LVDT), 3. Load cell, 4. Test pin, 5. Test flat, 6. Loading arm, 7. Guide rollers, 8. Housing for ball bearings which hold guideroller shaft.

FIG. 2. Schematic of the reciprocating sliding rig.

Si : 0–24%
Cu : 2–5%
Mg : 0.3–0.85%
Ni : 0–1%
Fe : 0.21%
Al : Rest

Specimens for mechanical and wear testing were machined out of the cast fingers. The counterface of EN24 was heat treated and ground to a finish of 0.5 μm CLA.

3. Results and discussion

3.1. *Wear classification*

There is a general agreement among various workers in this field that there are sharp wear transitions and the transition load increases with silicon content[3–14] .

Figure 3 shows the three possible regimes of wear—mild, severe and seizure. Figure 4 shows the same type of transitions to occur in reciprocating sliding as in unidirectional sliding, the general level of wear rate being however somewhat higher in the former than in the latter. Figure 5 shows typical worn surfaces belonging to the three regimes. The mild wear regime (Fig.5a) is characterized by delaminated craters and abrasive grooves. The severe wear surface (Fig. 5b) is very smooth; the contact with the counterface is intimate and there is extensive flow. The seized surface (Fig. 5c) shows a slab of material removed, spanning the pin diameter and leaving a heavily deformed surface. Figure 6 shows the mild wear rate and coefficient of friction to increase with sliding speed. Figure 6c shows the coefficient to decrease with alloying elements.

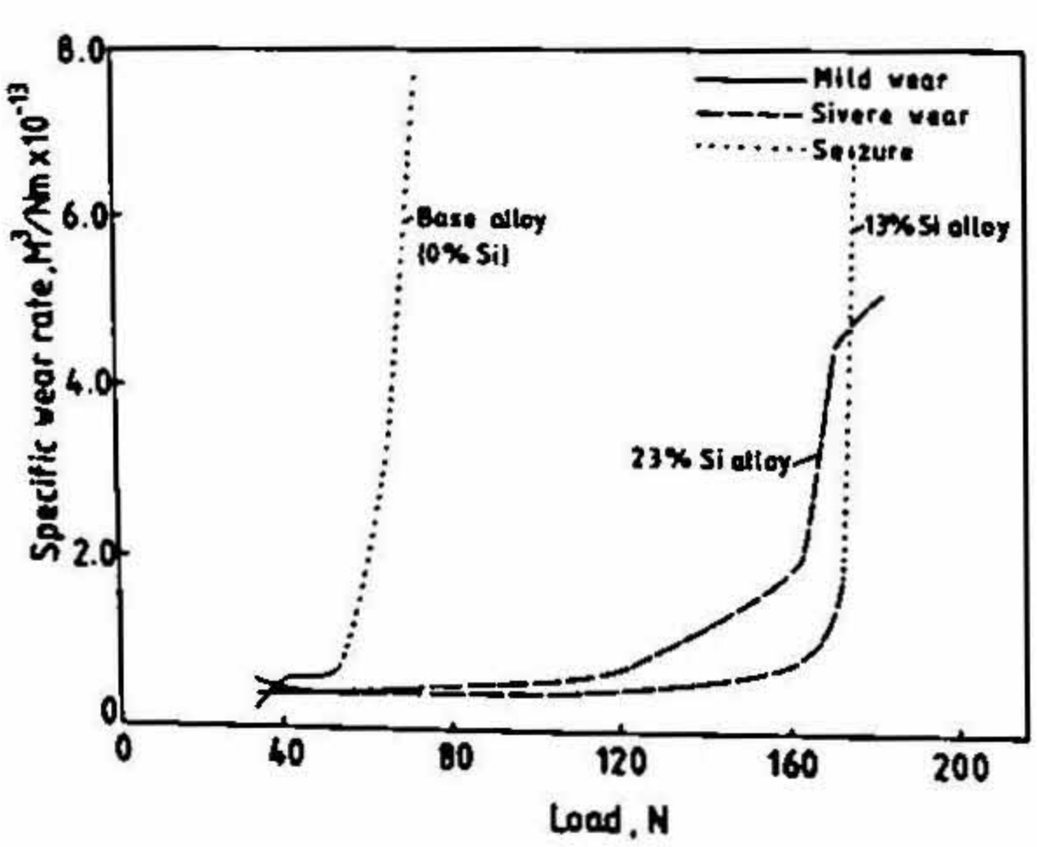

FIG. 3. Specific wear rate of test alloys demarcating three modes of wear—mild, severe and seizure.

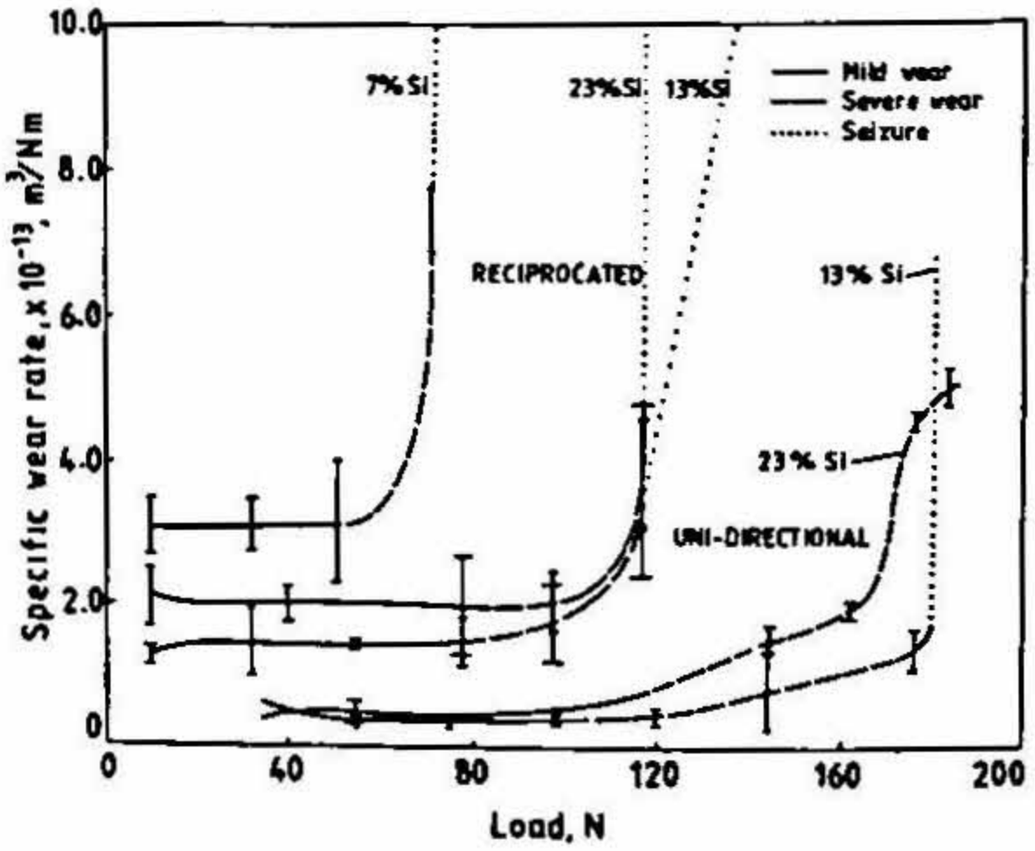

FIG. 4. Specific wear rate of binary alloys; unidirectional sliding at 0.8 m/s; reciprocating sliding at 0.6 m/s.

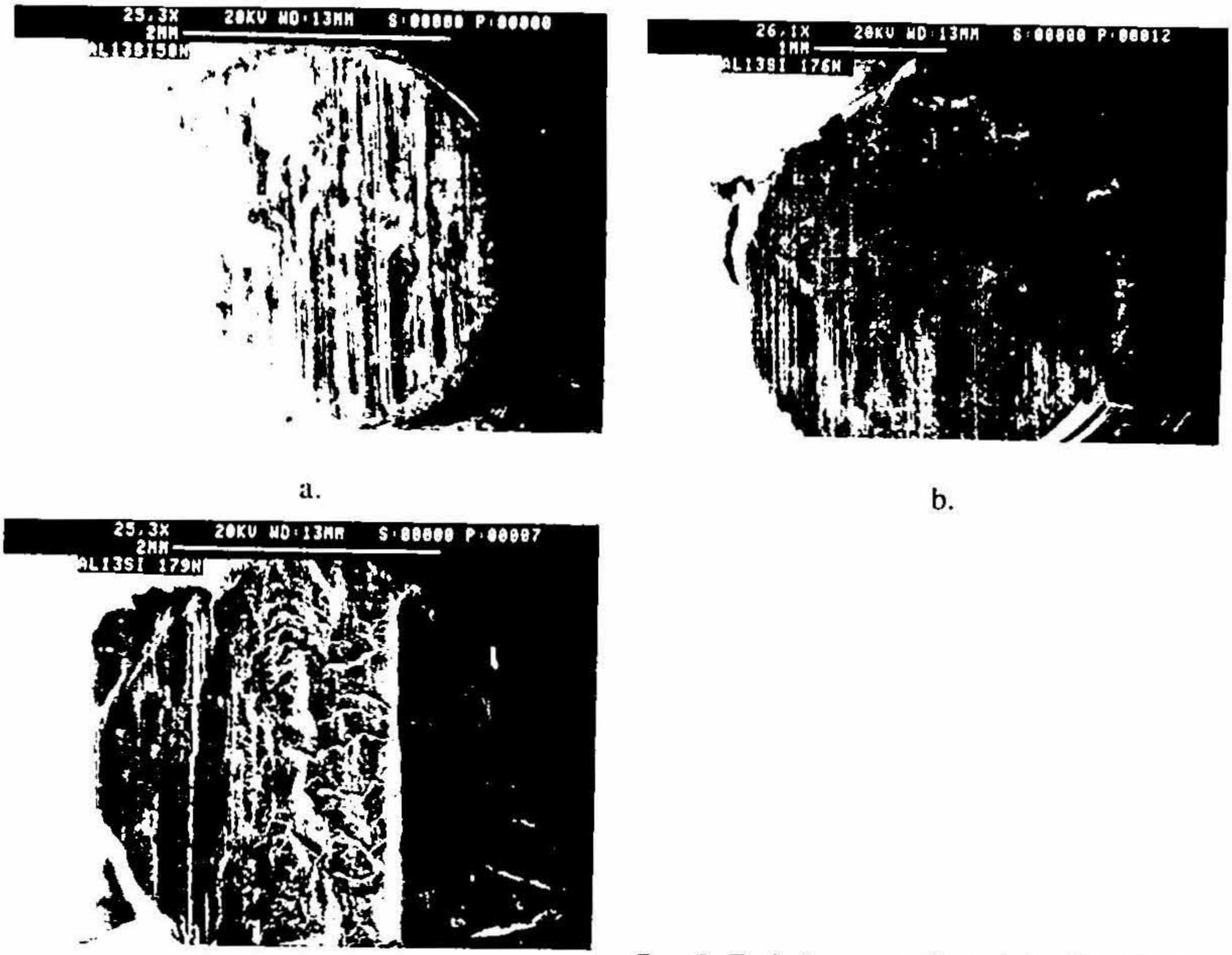

a. b. c.

FIG. 5. Typical worn surfaces belonging to three regimes of wear.

3.2. *Effect of silicon, alloying elements and heat treatment*

3.2.1. *Silicon*

The addition of silicon brings down the mild wear rate but further addition has very little effect (Fig. 6a). Considering the great controversy[8, 4, 20–32] on the effect of silicon content on wear, factorially designed experiments were conducted on the mild wear regime using binary alloys[7]. The results have revealed the following :

1. The wear of an alloy without silicon is significantly higher than that of binary alloys containing 4–24 wt% of silicon.
2. There is no systematic trend in the wear of alloys containing 4–24 wt% Si with respect to silicon content.
3. The wear rate increases linearly and monotonically with pressure.
4. The coefficient of friction is insensitive to variation in pressure, silicon content and speed.

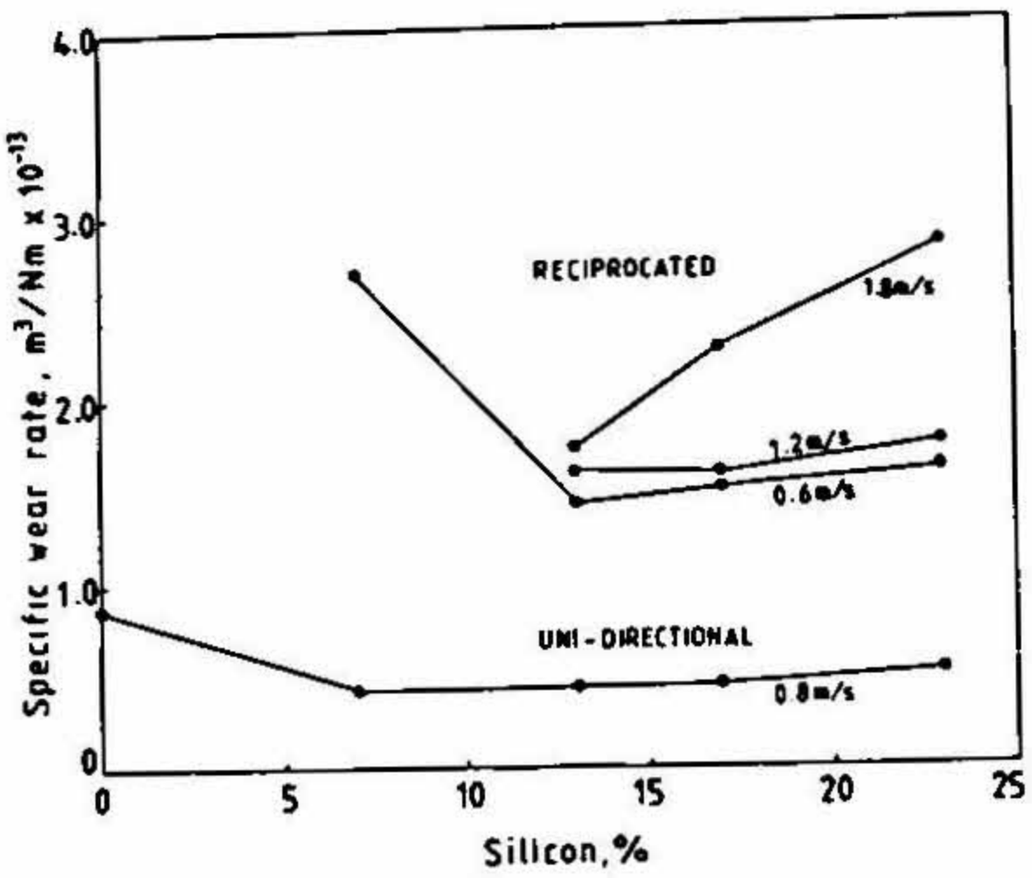

a.

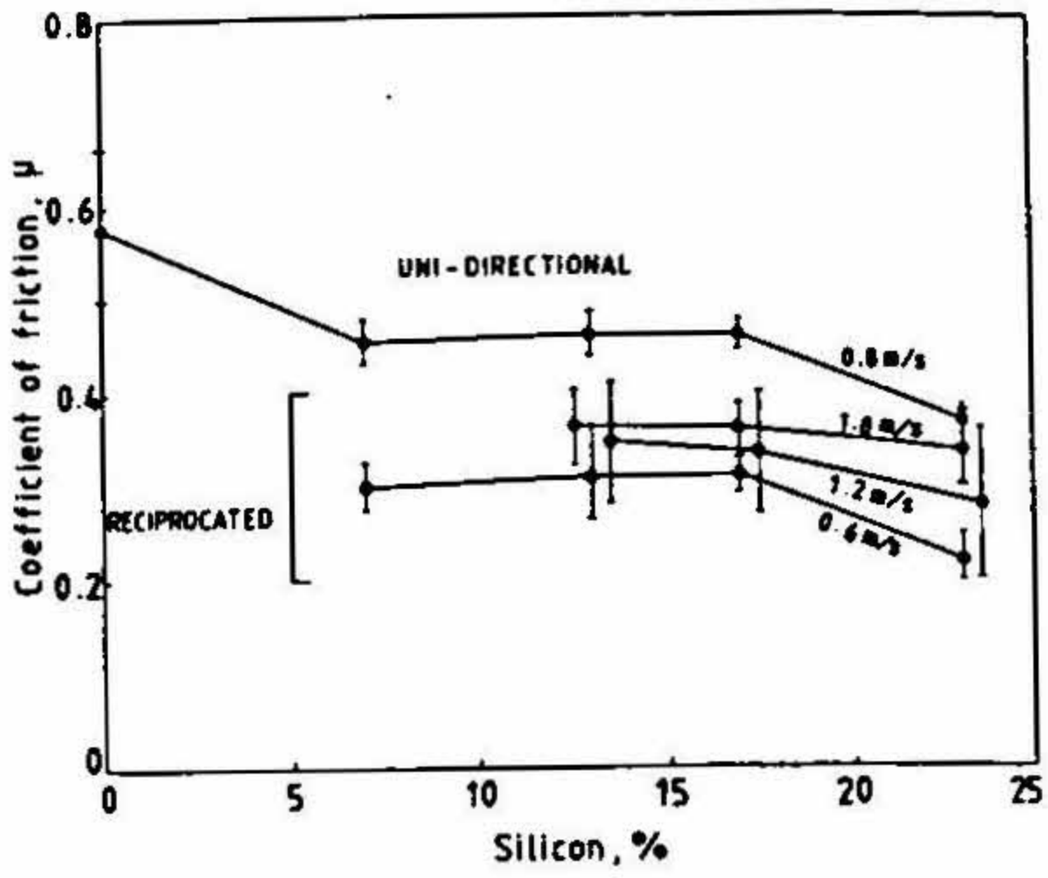

b.

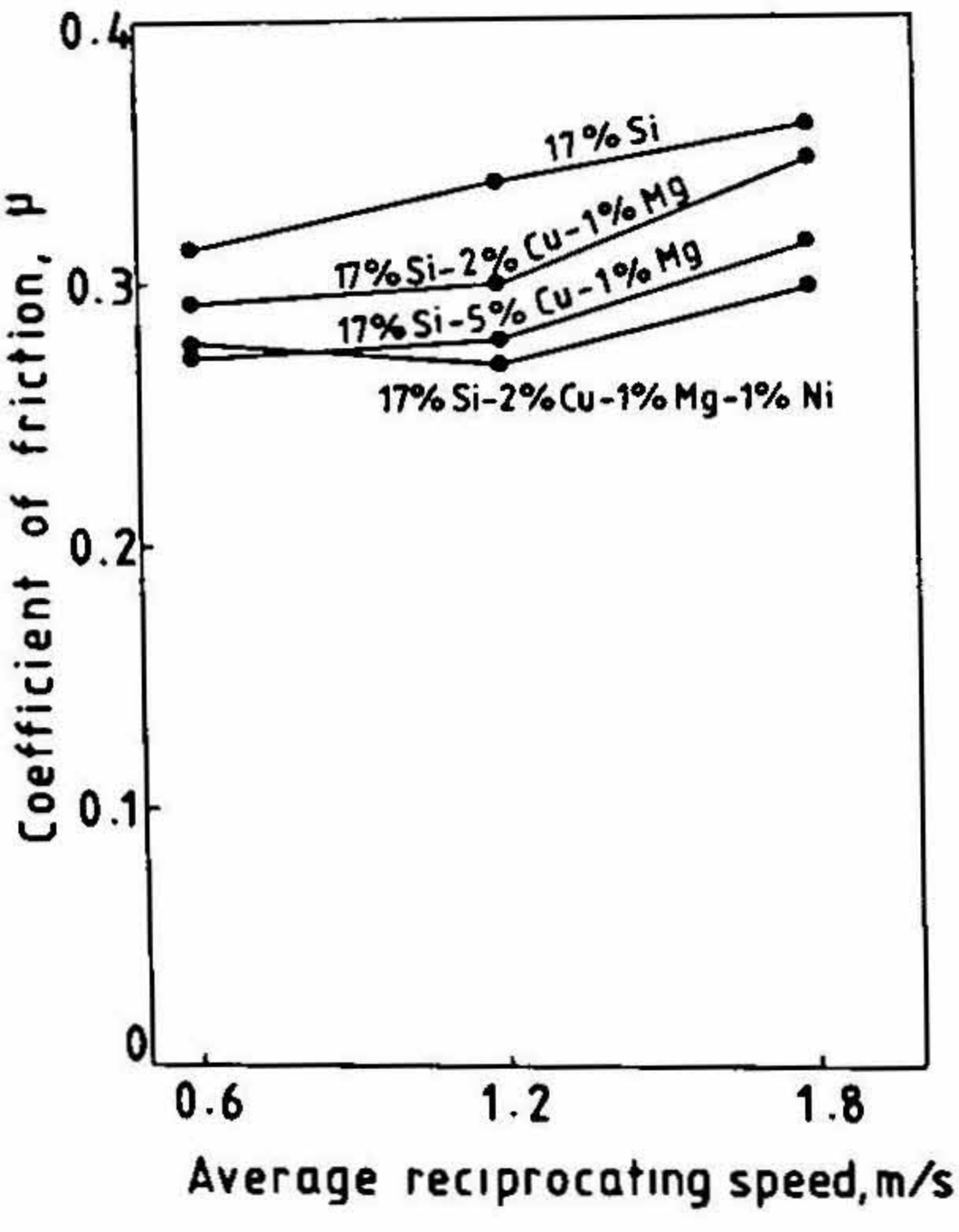

c.

FIG. 6a. Specific wear rate of binary alloys in the mild wear regime at different sliding speeds. b. Coefficient of friction of binary alloys in the mild wear regime at different sliding speeds. c. Coefficient of friction of Al–17Si alloys in the mild wear regime of reciprocating sliding.

The presence of silicon enhances the seizure load (in unidirectional sliding) substantially but as in the case of mild wear the actual silicon content has minimal effect[14] on the load up to 17% (Fig.7). Interestingly enough (see Fig. 7) within the present test load limit of 200 N the 23% silicon alloy never seized, while the 17% Si alloy seized 50% of the times tested. Under reciprocation[2], however, even 23% Si binary alloy seized and additions of silicon in the hypereutectic regime tended to lower the seizure load substantially

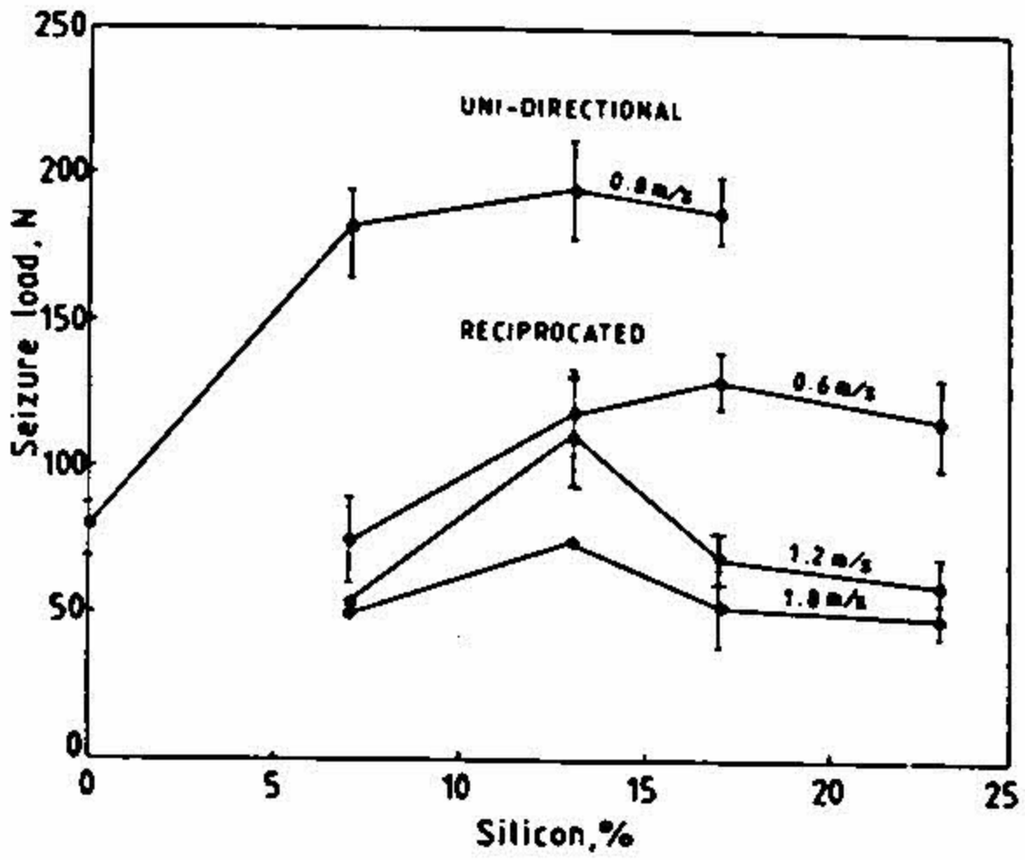

FIG. 7. The load (seizure load) at which seizure occurred for binary alloys.

when the reciprocating speed is high. From the point of view of seizure an eutectic alloy appears to give the best results under conditions of reciprocating sliding.

Additions of copper, magnesium and nickel to the alloy reduce the mild wear rate and enhance the seizure load (Fig. 8). When the magnesium content is high heat treatment of the alloy can make significant improvement in the mild wear resistance of the alloy (Fig. 9)[28].

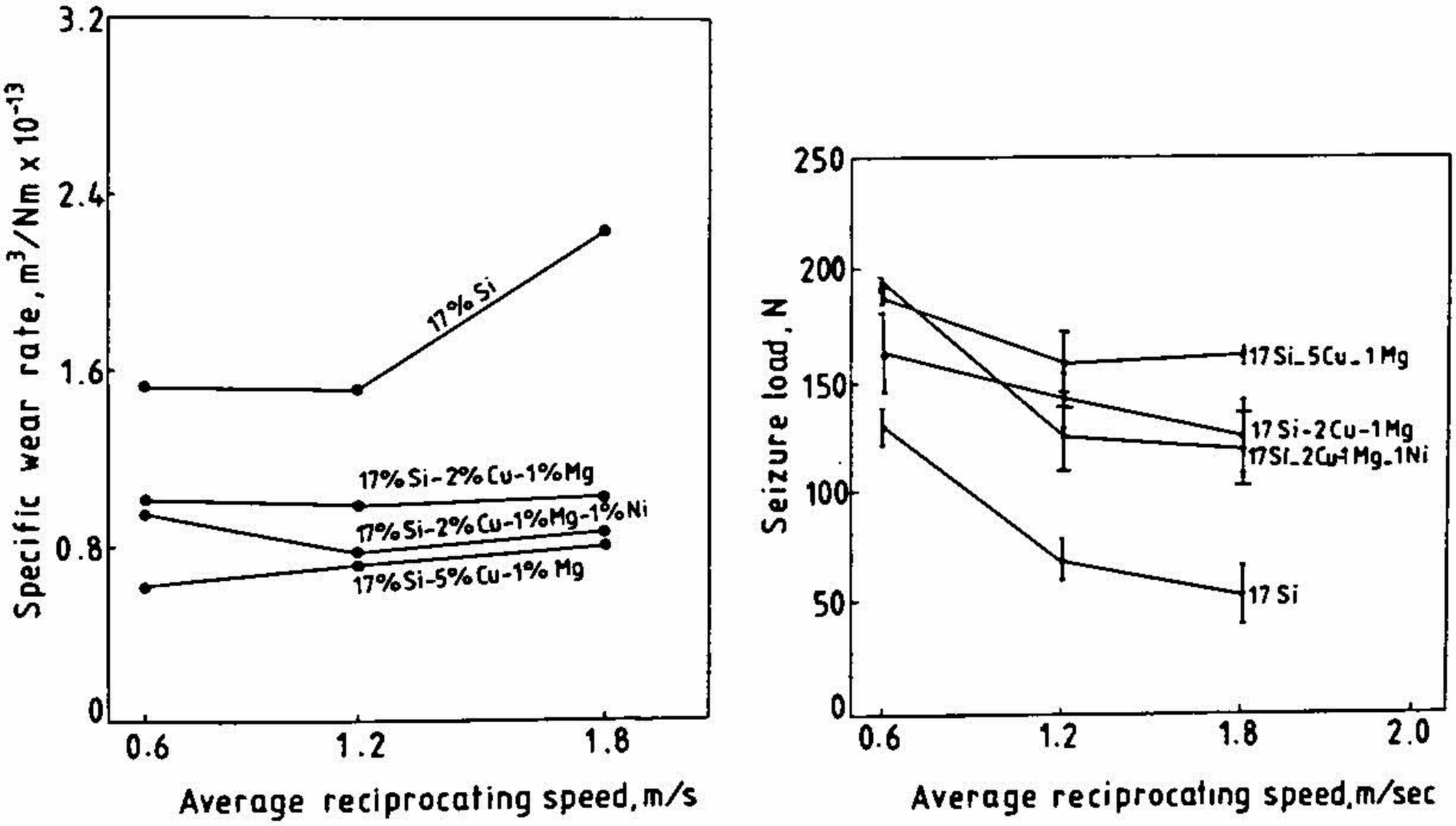

FIG. 8a. Specific wear rate of Al–17Si alloys in the mild wear regime of reciprocating sliding. b. The load (seizure load) at which seizure occurred for Al–17Si alloys in reciprocating sliding.

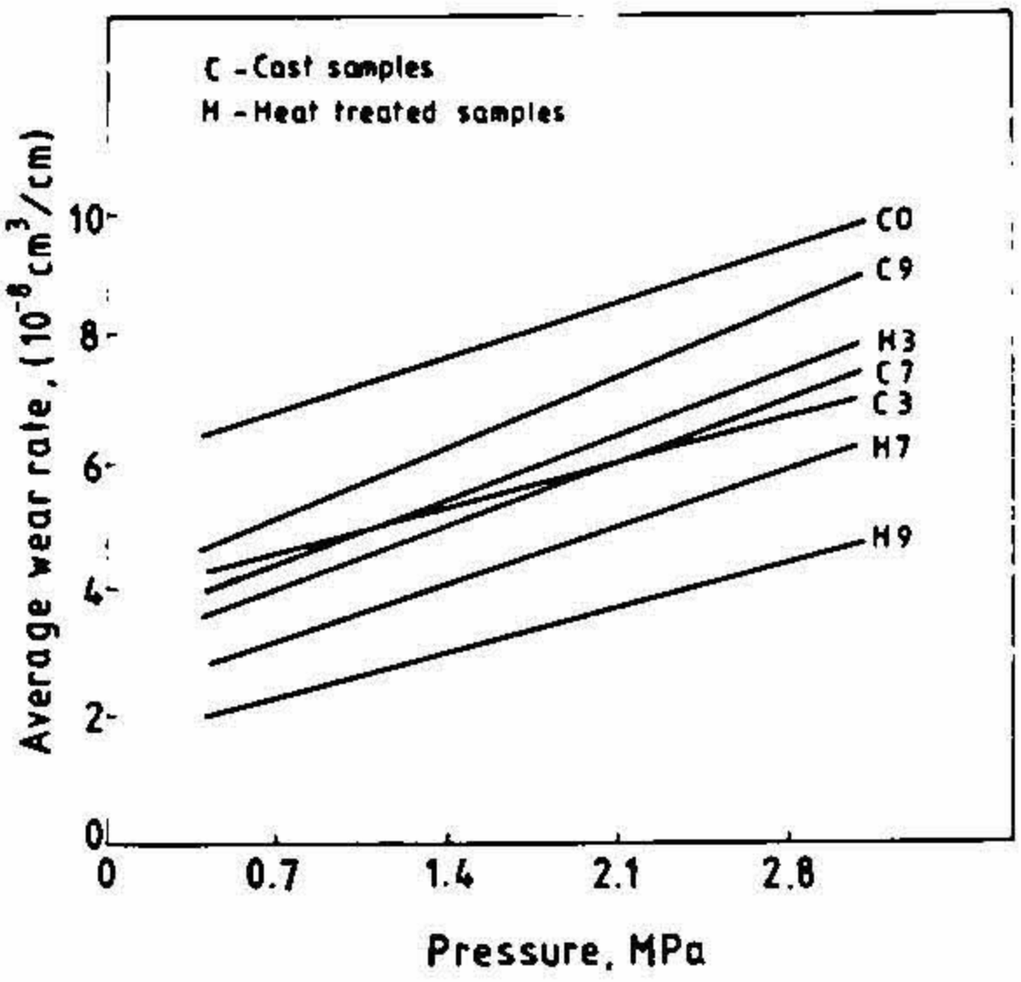

FIG. 9. Variation of wear rate of test alloys with pressure in different conditions.

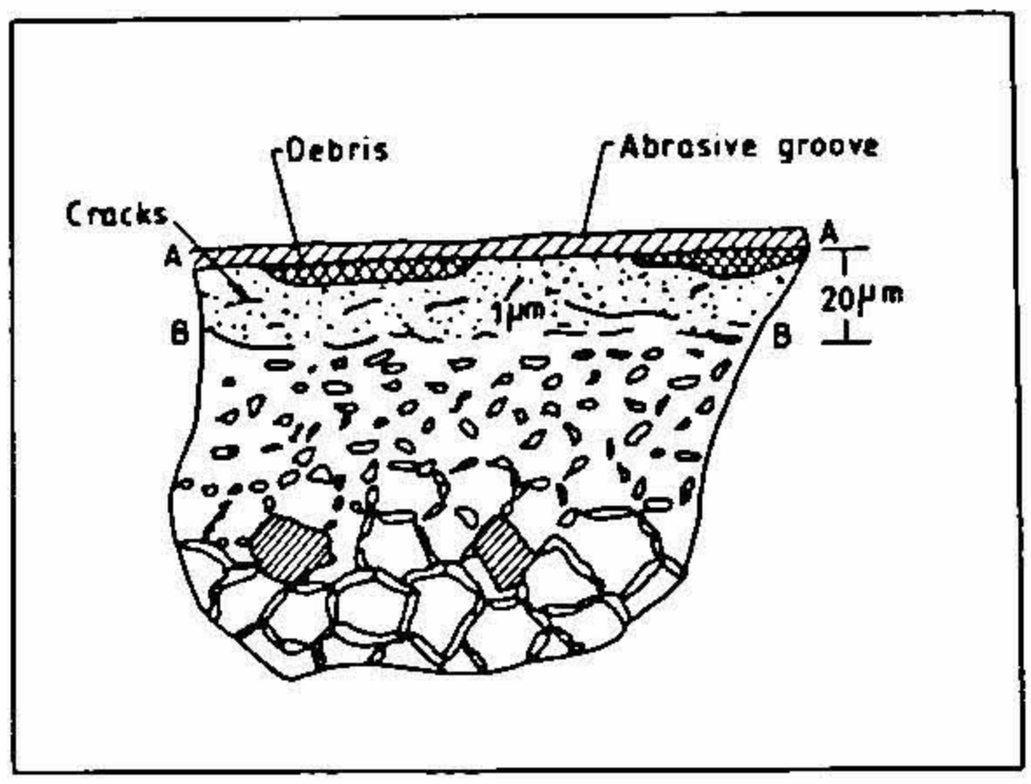

FIG. 10. Schematic diagram of the mild wear process.

3.3. *Mechanism of wear*

3.3.1. *Mild wear*

Mild wear is generally[29, 30] associated with oxidation where oxides are formed and compacted at the surface and get detached as debris. X-ray diffraction of the debris generated by a 12% Si[7] alloy under 2N load, however, showed the debris to be essentially metallic. Analysis of the surface of specimens worn in the mild wear regime, by SEM and EDXA, revealed the following features:

1. Actual SEM observations (Fig. 10) show the eutectic as well as the primary silicon fragment due to shear stresses generated in the subsurface due to traction. Figure 11 shows[31, 32] a possible mode of silicon fragmentation. As the strain increases in approaching the surface the size of the particle reduces till it becomes equiaxed and is about 1 μm

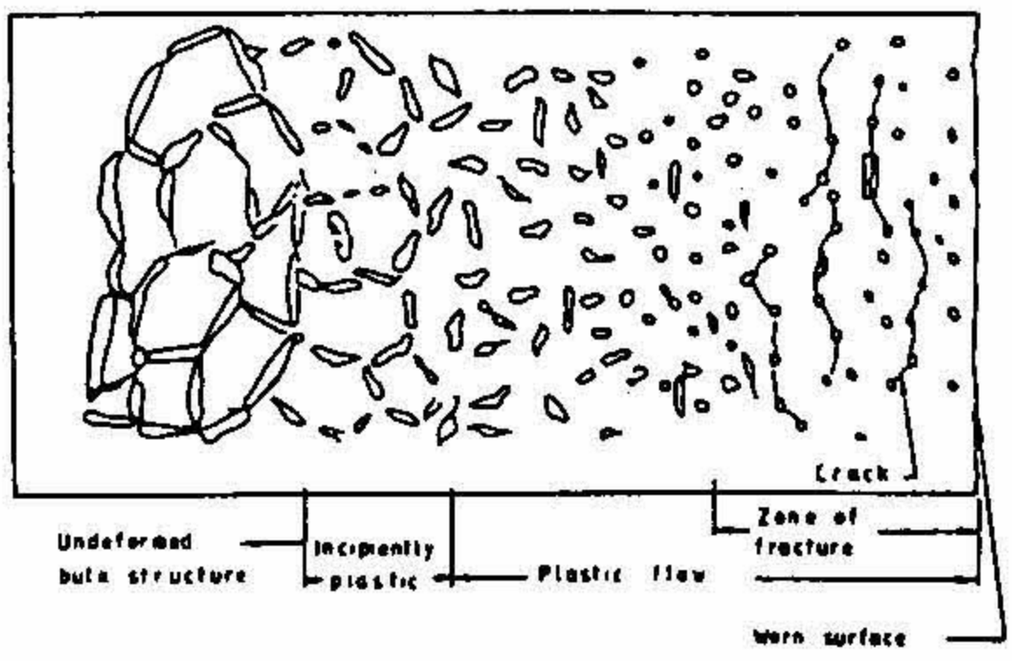

FIG. 11. Schematic of the proposed model of delamination wear.

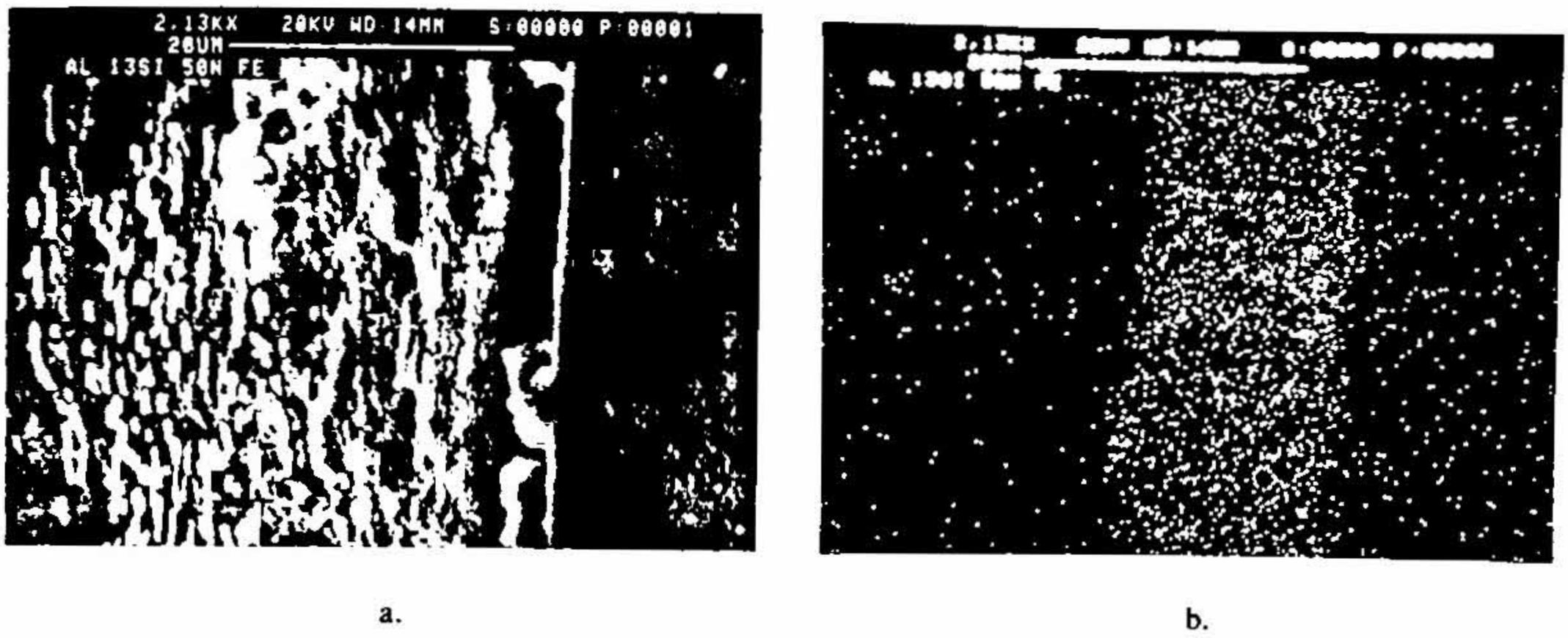

a. b.

FIG. 12a. Scanning electron micrograph of 13% Si subsurface worn in the mild wear region. b. X-ray dot mapping for iron corresponding to (a) showing the presence of an iron-rich protective surface layer.

diameter. Proceeding further towards the surface it becomes more difficult to fracture small particles than to nucleate a crack at the particle-matrix interface. These cracks once nucleated propagate in a direction parallel to the sliding plane in ultimately giving rise to laminate debris.

2. The surface zone consists of compacted debris from the alloy as well as the counterface. Figure 12 shows the Fe-map (EDXA) of the subsurface to indicate the existence of an iron-rich compacted layer[14].

3. The above layer is protective. If it can exist as a steady state without being destabilised the wear process remains in the mild region.

4. Stronger and more coherent the layer, lower the wear rate and more extensive the mild wear regime is. Greater strength and coherency of the protective layer is achieved by the addition of Cu and Mg and subsequent heat treatment[28]. Such treatment spherodises silicon and renders the matrix stronger. Figure 13 shows a nearly continuous smooth layer. There is little fragmentation of silicon below this layer (compare with Fig. 12). The abrasive resistance of the alloy increases by the alloy addition; the layer is difficult to destabilise and the spheroidal silicon particles discourage crack nucleation.The wear rate in the mild wear regime is low and the regime extends over wide bands of speed and load.

3.3.2. *Severe wear*

With increasing traction the subsurface stresses and temperature rise and the protective layer is destabilised. No protective compacted surface layer exists in the severe wear region[14]. The traction is directly transferred to the alloy subsurface as large stresses which are not high enough, however, to shear the whole surface. Instead, a thick band at the surface shows highly fragmented silicon and long cracks propagating parallel to the sliding direction (Fig.14). At the surface the temperature is high. The material flows

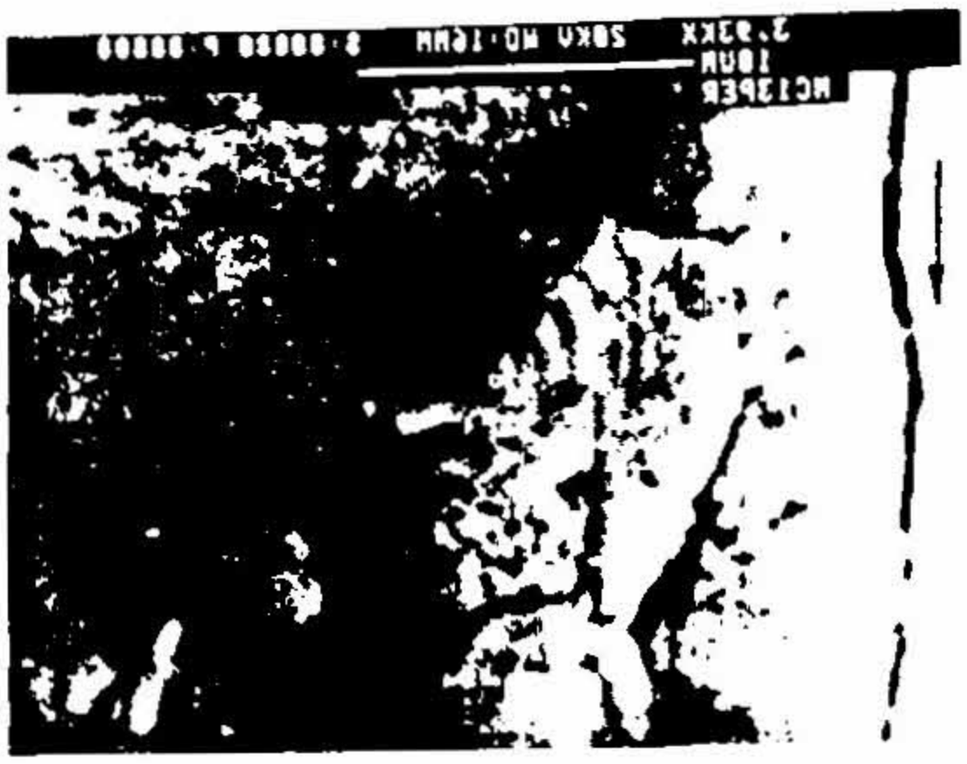

FIG. 13. A perpendicular section of Al-7 Si-0.85 Mg alloy in the heat-treated condition.

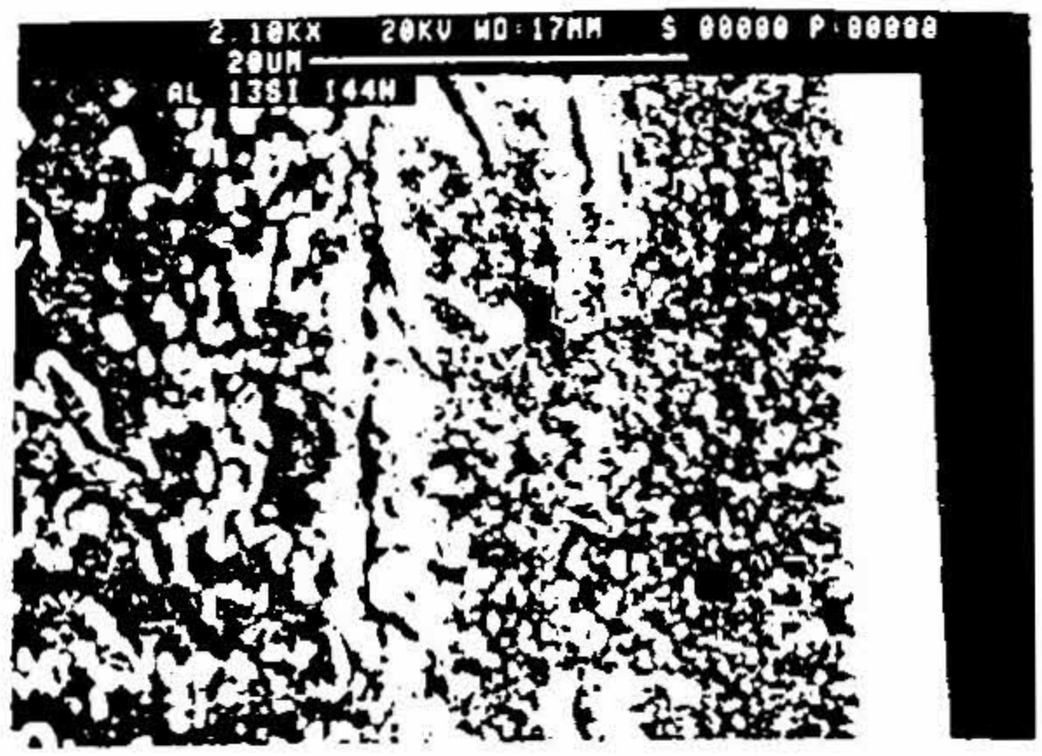

FIG. 14. Scanning electron micrograph of subsurface of 13% Si alloy specimen worn in the severe wear region showing deformed band containing highly fragmented silicon particles (size = 1 μm dia) and cracks propagating in this region.

under traction creating 100% contact between the alloy and the counterface. There is thus a dramatic rise in friction in this regime.

3.3.3. *Seizure*

For alloys, with silicon content up to about 17%, and the traction increased in the severe wear regions, large scale shear occurs in the subsurface in a plane parallel to the sliding direction and thick slabs extending across the pin diameter are dislodged.

3.3.4. *Anomalous behaviour of the 23% Si alloy*

The mechanics of material removal in the case of high silicon material is a study in contrast to that in the case of lesser silicon content materials. The absence of a protective layer in the mild wear region may be attributed to the propensity of this material to respond in an unstable manner when subjected to compressive loading. Such behaviour induces very high local strain rates. It has been postulated[8] that such high local strain rates in the immediate subsurface make it difficult for a stable layer to form.

The 23% Si alloy shows strain softening (Fig.15) and anomalous behaviour in room temperature compression. Such behaviour is associated with local instability such as shear bands and cracks. The 13% Si alloy, in contrast, shows (Fig.15b) strain hardening in compression and no microstructural instabilities. It is considered that the layered structure created by the crack (propagating parallel to each other and to the sliding direction) (Fig.16b) in the subsurface of a worn 23% Si specimen is a manifestation of the same instability. The silicon particles in this region are about 0.5 μm. This suggests that the strain and strain rates in this region of the subsurface are very high. Thus, as the material instability makes it impossible for the protective layer to form, direct contact is established between the test alloy and the counterface at all loads. The silicon particles present on the pin surface abrade the counterface. Iron particles are thus detected only

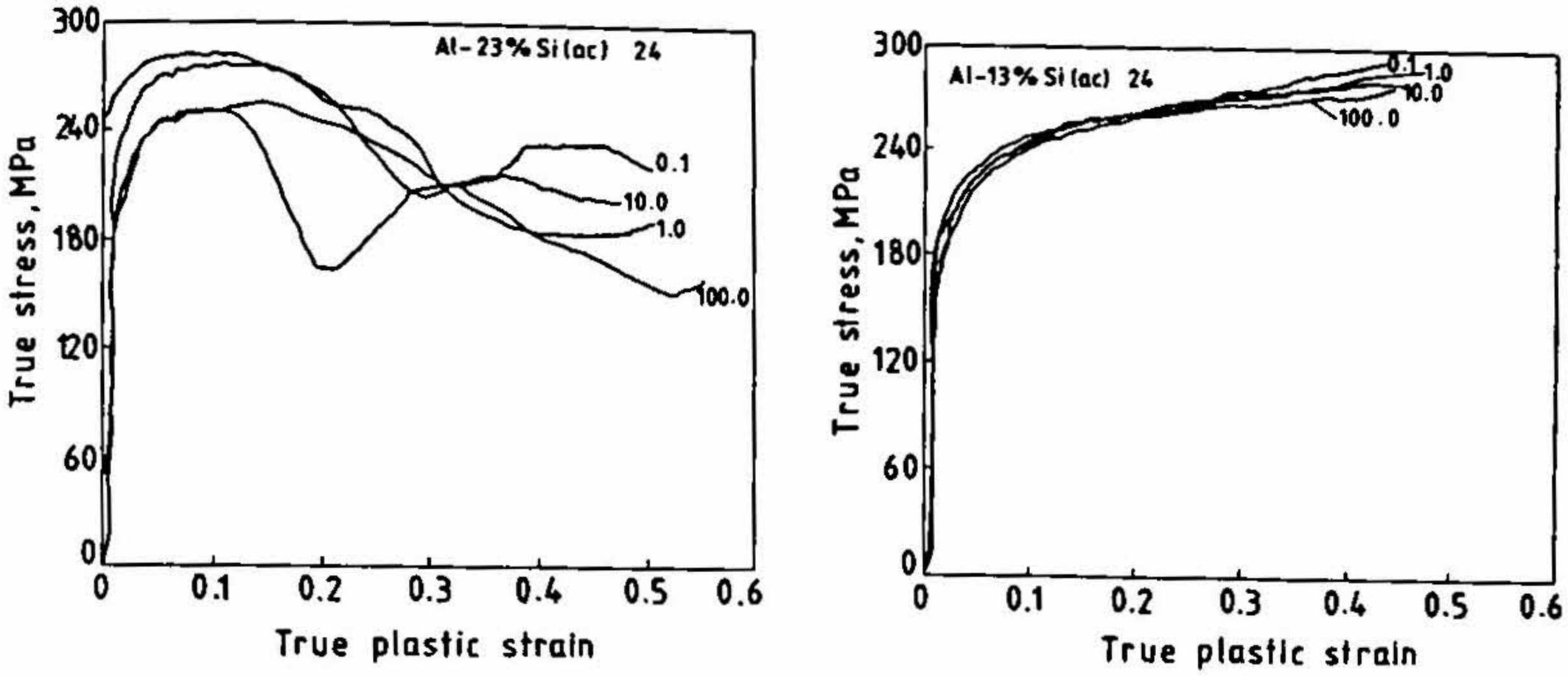

FIG. 15. Stress–strain behaviour in room temperature compression at various strain rates (0.1–100 s^{-1}). a. 23% Si alloy; b. 13% Si alloy.

on the surface and not in the subsurface (Fig.17). For the 23% Si alloys in the absence of a protective layer, the wear rate is marginally higher than other alloys in the low load regime and substantially higher than other alloys in the high load regime. While a weak and unstable subsurface of a 23% Si alloy specimen may be held responsible for the high wear rate of this alloy, the present results show that this weakness contributes little to the occurrence of seizure.

It may also be noted that the stress–strain behaviour of 17% Si alloy in compression has been found to be similar to but more stable than that of the 23% Si alloy. The surface and subsurface morphologies of specimens which seized in sliding were found to be very similar to those of the 13% Si alloys while the morphologies of the specimens which never seized were found to be similar to those of the 23% Si alloy specimen.

a. b.

FIG. 16. Scanning electron micrographs of a 23% Si alloy specimen worn in the severe wear region; a. low magnification view showing stratification and whirls within a 35 μm subsurface. b. higher magnification view of (a) showing the stratification as long cracks propagating parallel to the sliding direction.

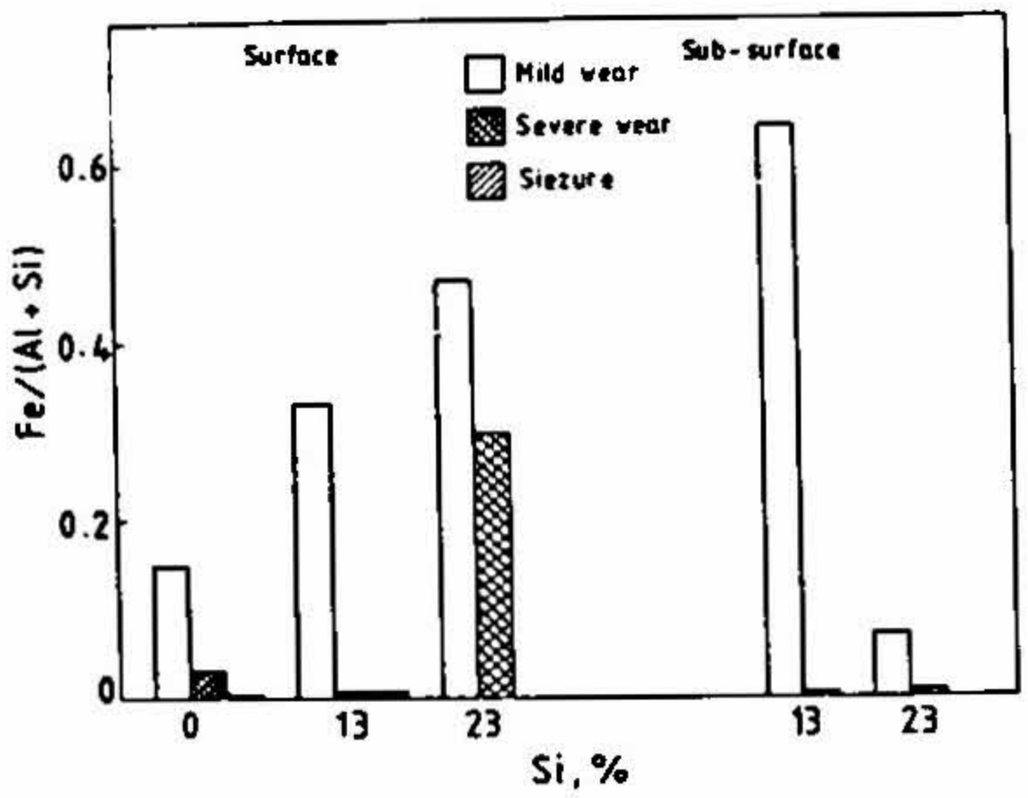

FIG. 17. Iron content of worn specimens as a function of silicon content, obtained using EDXA.

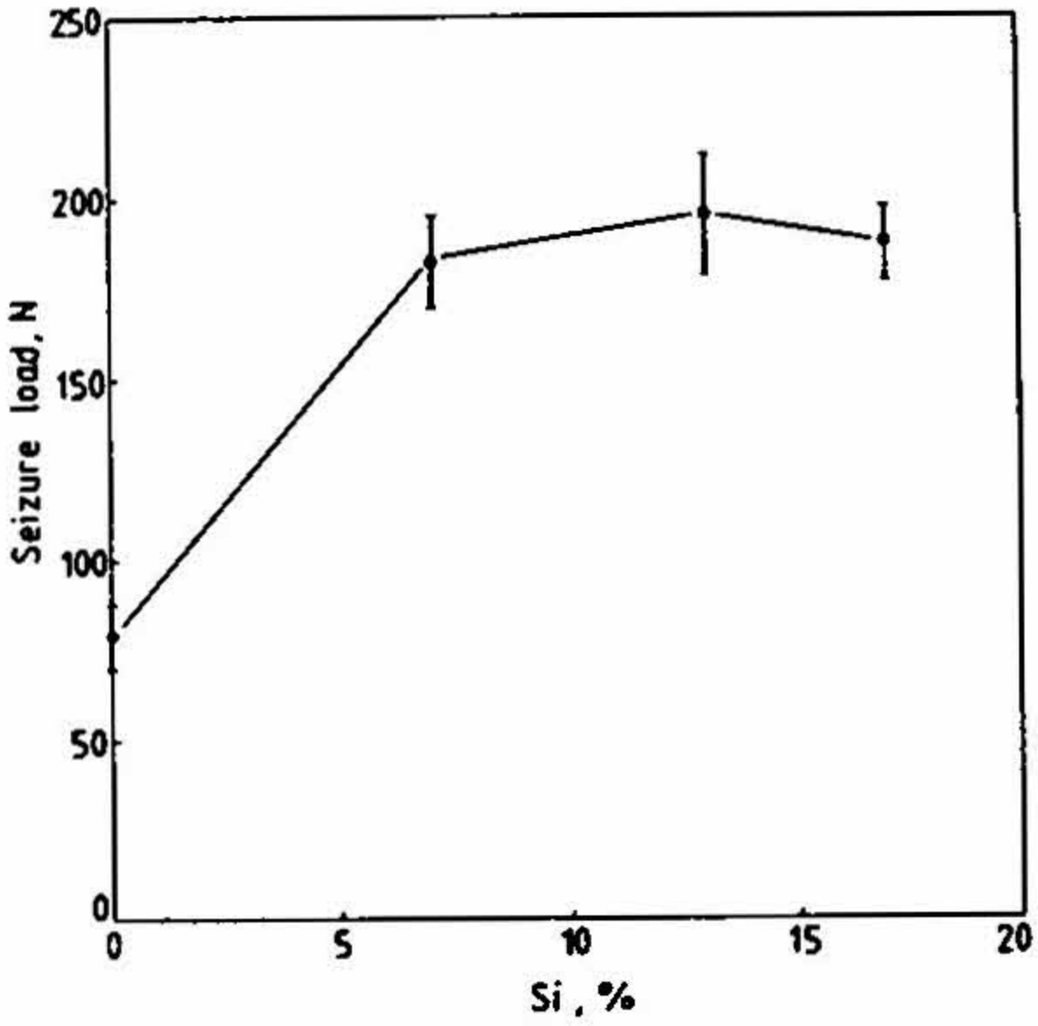

FIG. 18. Load at seizure of Al–Si alloys in unidirectional sliding as a function of silicon content, sliding speed, 0.8 m/s, 25°C.

3.4. *Mechanism of seizure*

Figures 7, 18, 19 show that

1. At low sliding speeds the addition of silicon increases the seizure load in unidirectional as well as reciprocating modes[2].
2. The seizure load decreases with sliding speed.
3. In unidirectional sliding, 23% Si alloy is highly seizure resistant. In reciprocating sliding at high speeds the seizure load for the hypereutectic alloy is low compared to the eutectic alloy[2].
4. Addition of alloying element enhances the seizure resistance of the alloys[1].

3.4.1. *Postulate*

To account for the above results it is postulated that there exists a temperature for a material at which gross plastic flow criterion of shear stress/hardness (0.2–0.166) is satisfied at a subsurface depth. When this happens the material seizes and gross shear takes place at this depth in a plane parallel to the sliding plane.

3.4.2. *Analysis*

If s is the adhesive component of the shear stress experienced in an isothermal scribing it is possible to deconvolute this from the measured tangential force. Figure 20 shows that when s/p, where p is the hardness at a temperature, is plotted against temperature the seizure criterion is always satisfied for an alloy with no silicon. The temperature at

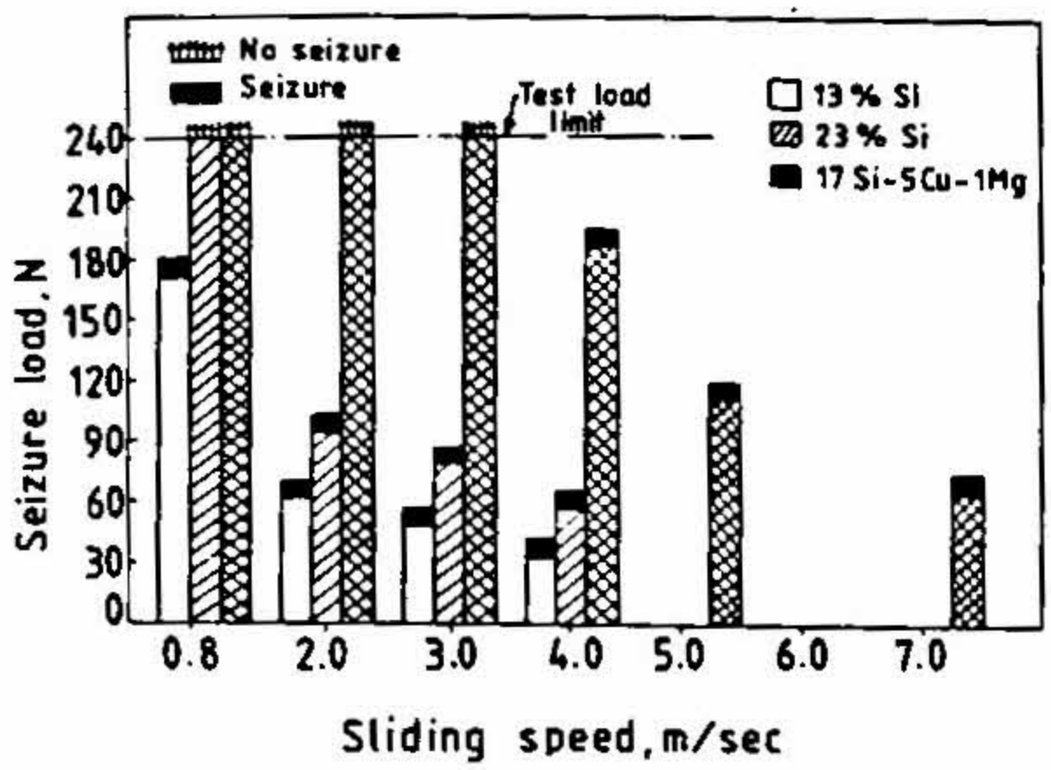

FIG. 19. Load at seizure of test alloy as a function of sliding speed, 25°C .

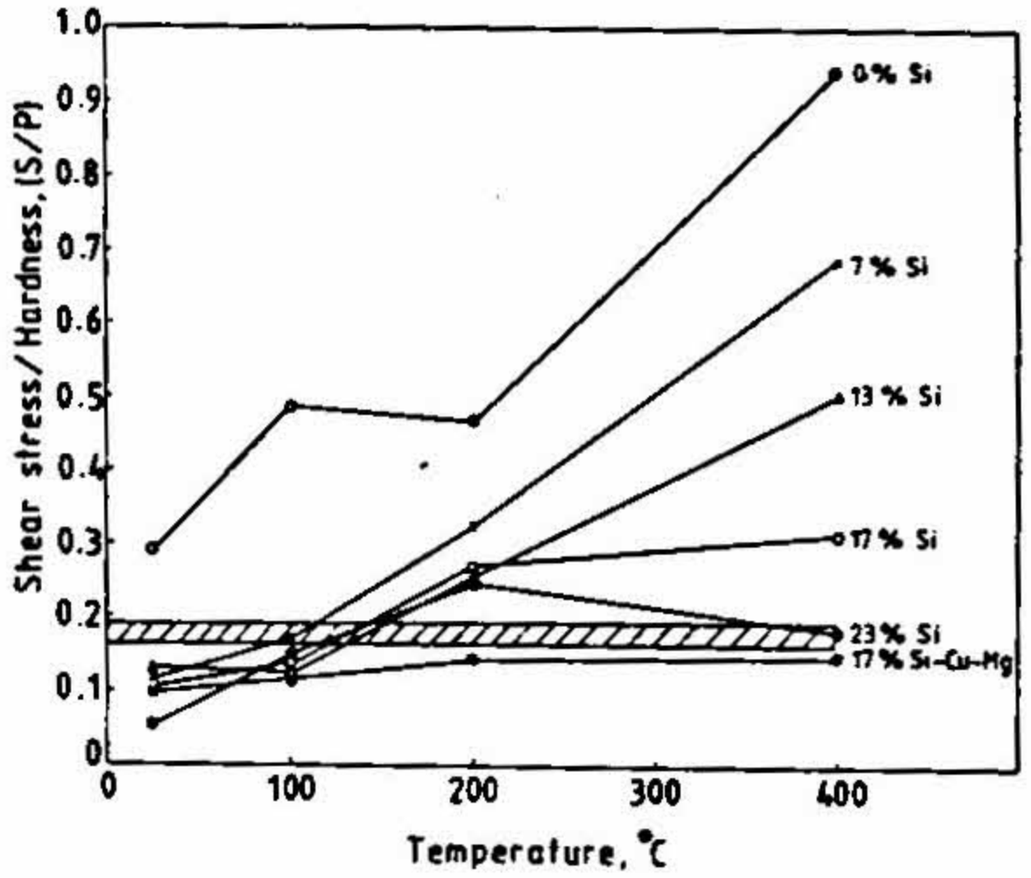

FIG. 20. Shear stress–hardness (s-p) ratio of test alloys as a function of temperature as obtained using scribing test data, sliding speed, 3×10^{-5} m s^{-1} .

which the criterion is satisfied for other alloys appears to increase with silicon content. When copper and magnesium are added to the binary alloys the criterion is not satisfied even up to 400°C.

This argument is now extended to the sliding wear tests and an s/p ratio is computed. If s is assumed to remain constant with temperature, Fig. 21 shows that the seizure criterion for 0% Si alloy is satisfied at the lowest temperature. The seizure temperature increases with the silicon content so much so that the 23% Si alloy does not seize even at 400°C.

This model has the following implications which appears to agree with the observation on seizure made earlier. Increasing the silicon content pushes the seizure temperature up. This means that the addition of silicon requires an increase in load or speed or

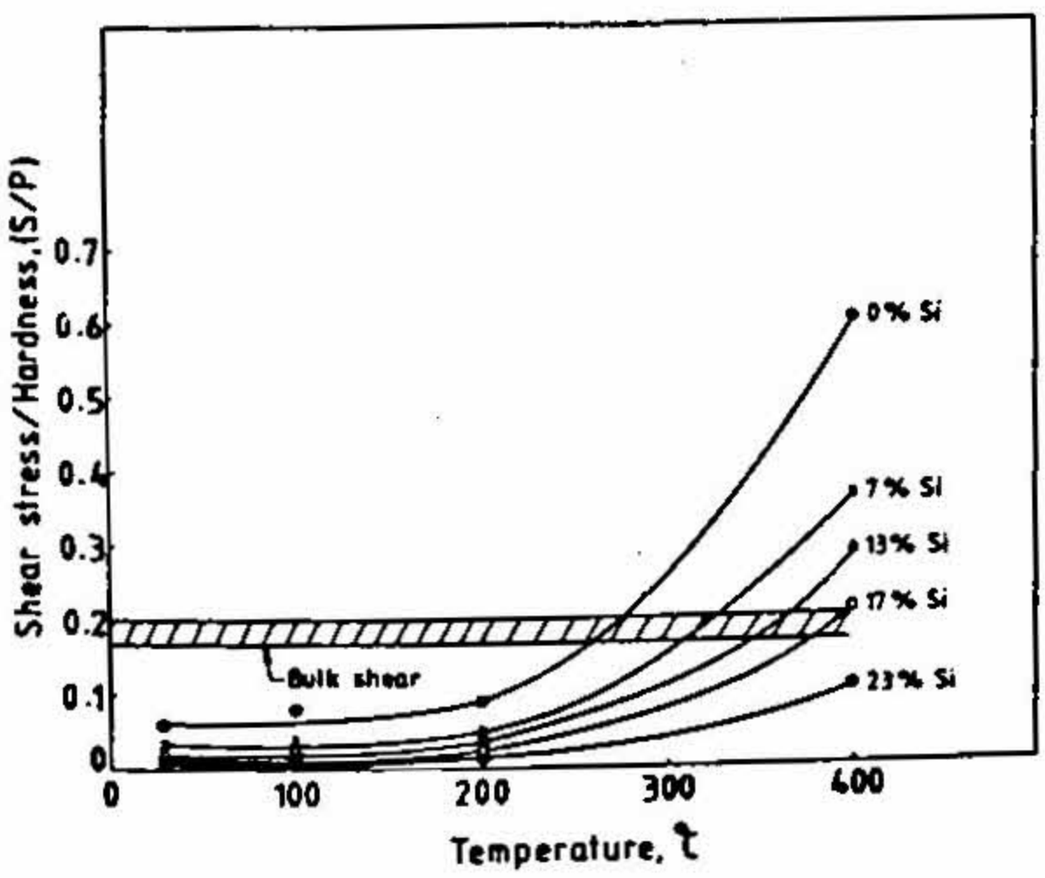

FIG. 21. Shear stress–hardness (s-p) ratio of different test alloys as a function of temperature in unidirectional sliding, sliding speed, 0.8 m s^{-1} .

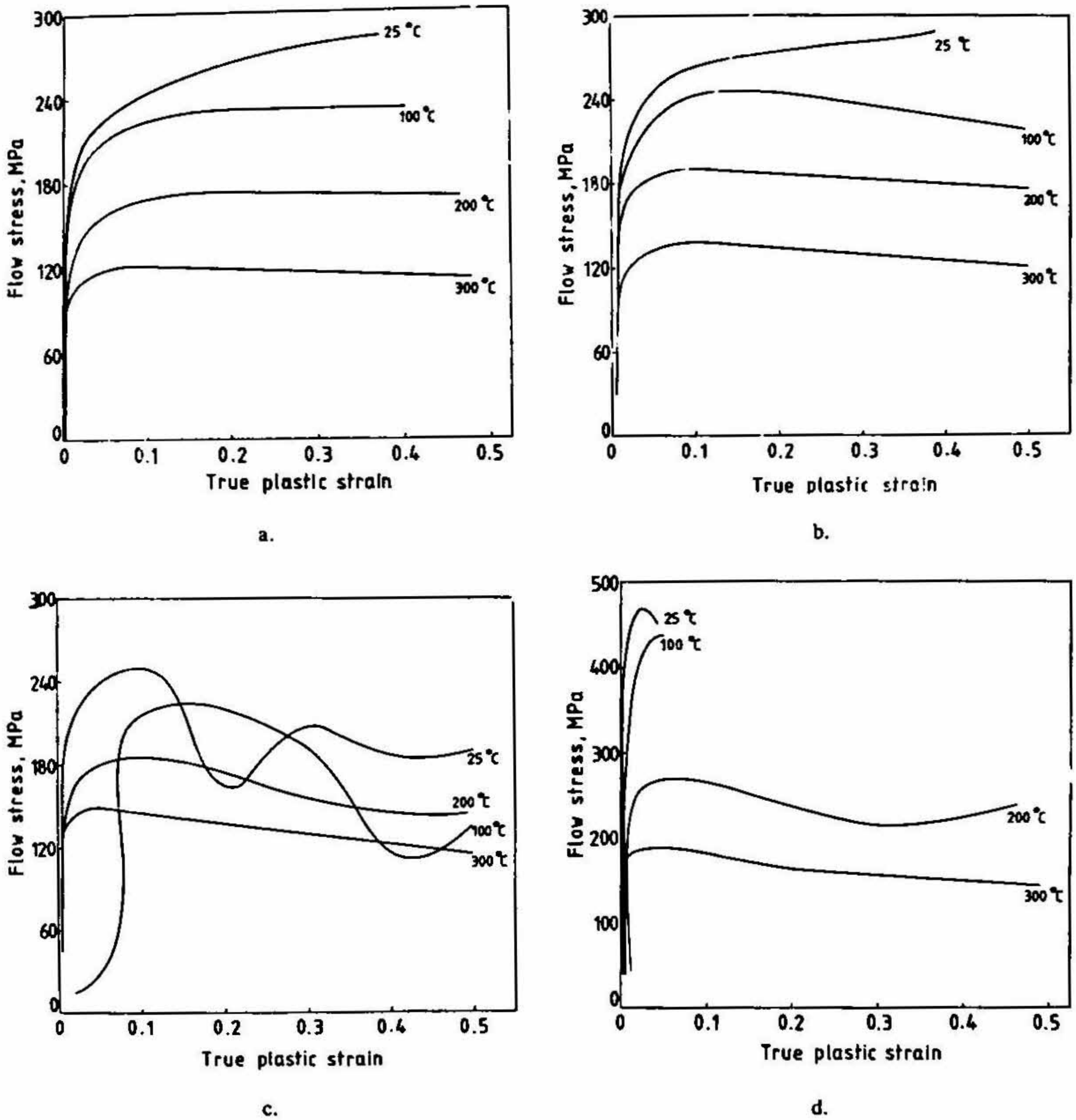

FIG. 22a. Stress–strain behaviour of Al-13 Si binary as cast alloy in uniaxial compression at a constant strain rate of 1 m s^{-1}. b. Stress–strain behaviour of Al-17 Si binary as cast alloy in uniaxial compression at a constant strain rate of 1 m s^{-1}. c. Stress–stress behaviour of Al-23 Si binary as cast alloy uniaxial compression at a constant strain rate of 1 m s^{-1}. d. Stress–strain behaviour of Al-17Si-2Cu-1Mg as cast alloy in uniaxial compression at a constant strain rate of 1 m s^{-1}.

both to yield the higher subsurface temperature required to bring the new material to the point of seizure. The argument may be extended to the addition of alloying elements.

Figure 7 shows that the seizure load decreases as the operating mode is changed from unidirectional to reciprocating and decreases further when the reciprocating speed is increased. When alloying additions are made the friction coefficient decreases (Fig. 6c)

from that of the base alloy but the strength increases (Fig. 22) considerably. The addition of alloying elements would thus reduce the s/p ratio. Figure 8b shows that the seizure load for the 17Si–5Cu–1Mg alloy in reciprocating sliding is significantly higher than that for the base alloy reciprocated at the same speed.

The variation of seizure load with silicon content is rationalized for unidirectional sliding, using the argument given above. Figure 7 shows that at a low speed (0.6 m/s), while the seizure load is lowered by changing the sliding mode from unidirectional to reciprocating, the trends in the seizure load with silicon content remain substantially the same. It is interesting to note, however, that when the average speed is raised to 1.2 and 1.8 m/s the seizure load for the hypereutectic alloys, instead of remaining more or less unchanged (as in the case of unidirectional sliding at 0.8 m/s or reciprocating sliding at 0.6 m/s), reduces drastically with increasing silicon content. The reason for this may be related to the unstable microstructural responses of these hypereutectic alloys to the specific strain rates and temperatures generated in the subsurface during sliding. Flow softening and unstable stress–strain behaviour of a material at a given strain rate and temperature are generally indicative of characteristic unstable microstructural responses to the operative strain rate at the test temperature. In uniaxial compression (0.1–100 s^{-1} strain rate) Al-17Si binary alloy starts to exhibit (Fig. 22b) flow softening, even at 100° C. Al-23Si alloy shows (Fig. 22c) flow softening and unstable stress-strain behaviour,

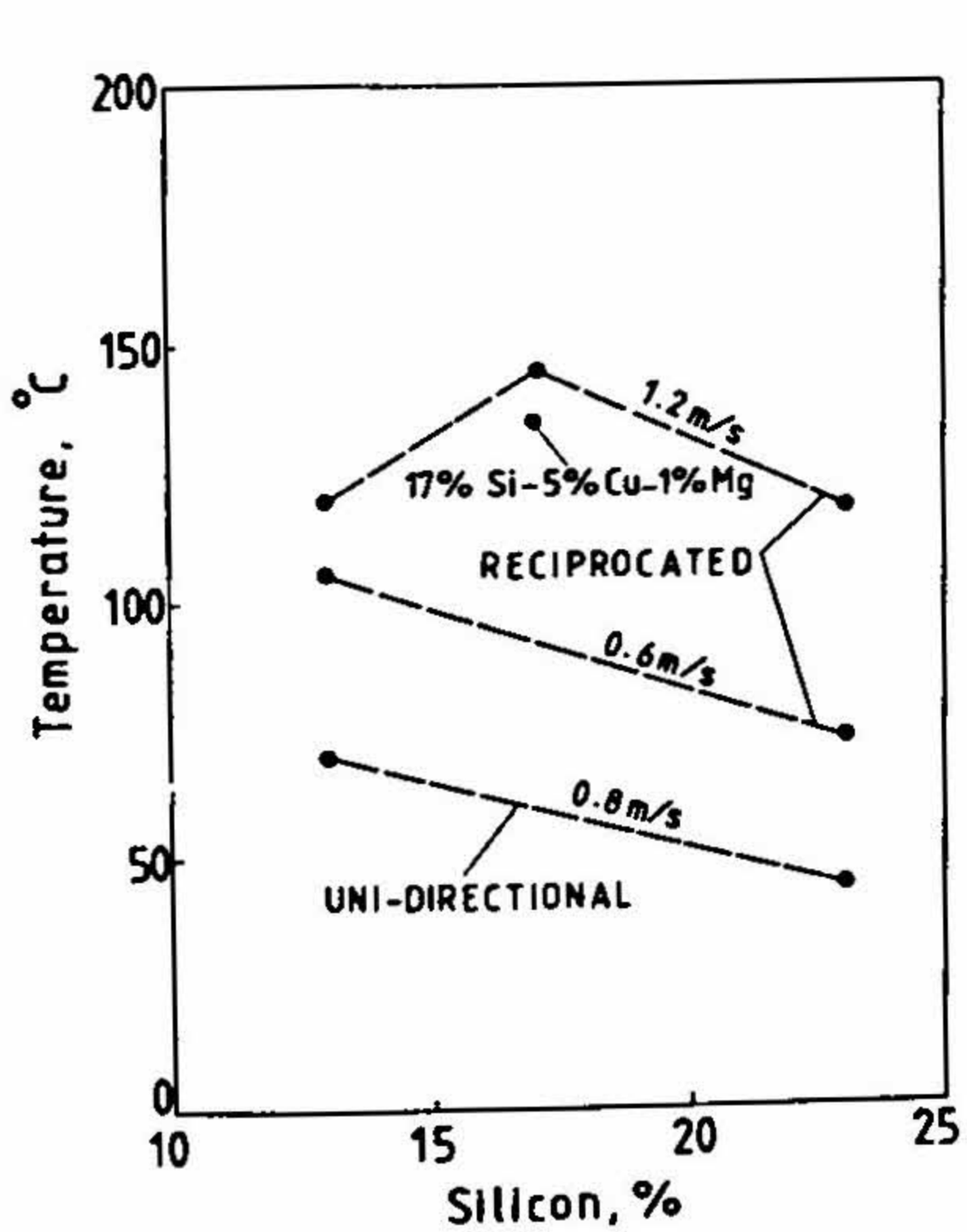

FIG. 23. Temperature rise in 9-mm diameter specimens in the mild wear regime. The temperature was recorded by a thermocouple tip inserted through a 1-mm diameter radial hole up to the pin axis, at a distance of 1.5 mm from the pin surface.

even at room temperature. In contrast, hypoeutectic alloys show a much more stable response (Fig. 22a) to uniaxial compression in the temperature range 25–300°C and strain rate of 0.1–100 s^{-1}.

Figure 23 shows that when the average reciprocating speed is 0.6 m/s, the subsurface temperature of the hypereutectic (23% Si) alloy is about 70% of that of the eutectic (13% Si) alloy . The difference is due to the low coefficient of friction (Fig. 6b) of the 23% Si hypereutectic alloy. What is curious, however, is that in spite of this the hypereutectic alloy seizes at about the same load (Fig. 7) as the eutectic alloy when the sliding speed is low. The reason for this may be because the hypereutectic alloys exhibit flow softening and unstable microstructural behaviour such as adiabatic shear banding, even

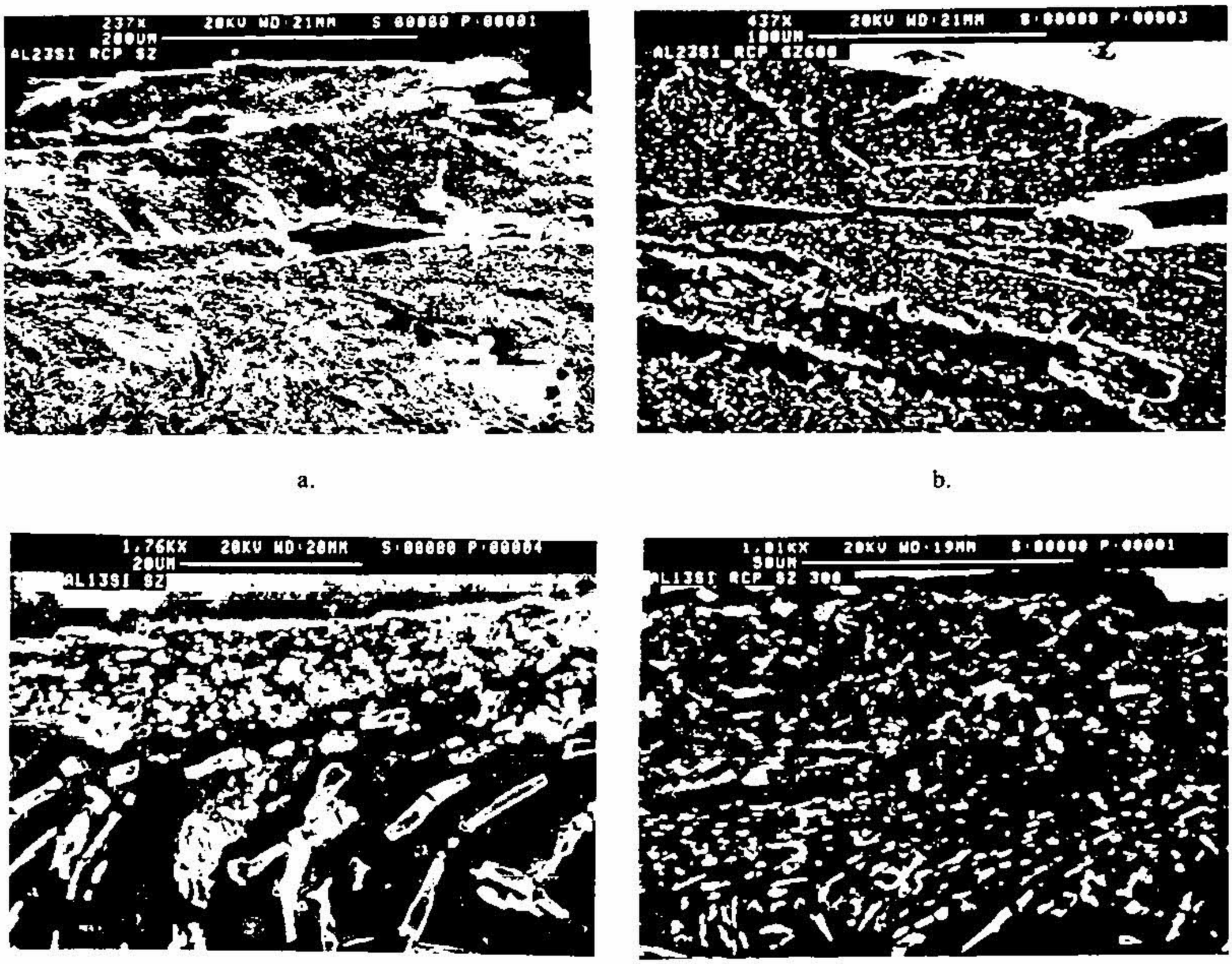

FIG. 24a. SEM micrograph of the subsurface of a seized sample generated in reciprocating sliding. Al–23Si binary alloy. 0.6 m/s sliding speed. Note the different directions of crack propagation in adjacent stratified layers. b. SEM micrograph of the subsurface of a seized sample generated in reciprocating sliding. Al-23 Si binary alloy. 1-2 m/s sliding speed. Note the different directions of crack propagation in adjacent stratified layers. c. SEM micrograph of the subsurface of a seized sample generated in unidirectional sliding; Al-13 Si binary alloy, 0.8 m/s sliding speed. Note the absence of a surface layer. d. SEM micrograph of the subsurface of a seized sample generated in reciprocating sliding. Al-13Si binary alloy 0.6 m/s sliding speed. Note the absence of a surface layer and the presence of subsurface cracks.

at relatively modest temperatures. Such shear banding and associated cracking (Fig. 24a) would encourage bulk shear, the phenomenon associated with seizure. Increasing the sliding speed to 1.2 m/s brings the hypereutectic subsurface temperature to a level that is about the same as that of the hypoeutectic alloy (Fig. 23). This would clearly encourage load. Figure 24b shows subsurface cracks propagating along the flow direction in a more widespread instability in the subsurface and the consequent lowering of the seizure highly deformed subsurface of a 23% Si alloy reciprocated at 1.2 m/s. Such deformation, shear and fracture were not observed in seized hypoeutectic samples (Figs 24c and d).

4. Conclusions

To retain an aluminium–silicon alloy piston in the lowest wear regime it is important that a stable iron-rich compacted tribo-layer forms at the interface. The addition of alloying elements, such as copper and magnesium, and subsequent heat treatment makes this layer coherent and strong. The addition of these elements lowers the wear rate in the mild wear regime as well as delays (w.r.t load and speed) transition to severe wear regime. It appears to matter only marginally as to what the silicon content is as long as there is some silicon, as long as other alloying elements can be added and as long as the alloy is responsive to heat treatment.

Actual silicon content, on the other hand, appears to make a great deal of difference as to the seizure potential of the alloy. The addition of silicon and alloying elements enhances the temperature at which seizure is likely to occur. At a given combination of the speed of the engine and the constant pressure acting on a piston groove, for example, increase in silicon content and alloying addition would reduce the probability of seizure. This is true up to the eutectic alloy. At higher content of silicon the unstable high strain rate response of the hypereutectic alloys increases the probability of seizure. From the point of view of seizure scuffing a heat-treated eutectic alloy (11–13% Si) with Cu and Mg would give the best performance.

Acknowledgments

The work reported here is the summary of over 15 years of work in the authors' laboratory. The names of persons who have helped is too numerous to enlist. H.S. Shamsunder has helped throughout in this work. Financial grants received (by SKB) from the Department of Science and Technology (DST), Council for Scientific and Industrial Research (CSIR) and the Department of Mines, Govt. of India, during the period of this study, are acknowledged.

References

1. Somi Reddy, A., Murthy, K. S. S. and Biswas, S. K. — Mechanism of seizure of aluminium–silicon alloys dry sliding against steel, *Wear*, 1995, **181–183**, 658–667.

2. Somi Reddy, A., Murthy, K. S. S. and Biswas, S. K. — Wear and seizure of aluminium–silicon piston alloys in reciprocating motion against steel, *Proc. Instn Mech. Engrs, J. Engng Tribol.*, 1995, **29**, 287–296.

3. SHIVANATH, R., SENGUPTA, P. K. AND EYRE, T. S. — Wear of aluminium–silicon alloys, *Br. Foundryman*, 1977, **70**, 349–356.

4. SARKAR, A. D. (ED.) — Wear of aluminium–silicon alloys. In *Wear of metals*, 1976, pp. 148–153, Pergamon Press.

5. ANDREWS, J. B., SENEVIRATNE, M. V., ZIER, K. P. AND JETT, T. R. — The influence of silicon content on the wear characteristics of hypereutectic Al–Si alloys, *ASME Int. Conf. on Wear of Materials*, 1985, pp. 180–186

6. EYRE, T. S. — Wear of aluminium alloys, *Microstruct. Sci.*, 1980, **8**, 141.

7. PRAMILA BAI, B. N. AND BISWAS, S. K. — Effect of load on dry sliding wear of aluminium–silicon alloys, *ASLE Trans.*, 1986, **29**, 116–120.

8. KRISHNA KANTH, V., PRAMILA BAI, B. N. AND BISWAS, S. K. — Wear mechanisms in hypoeutectic aluminium–silicon alloys sliding against steel, *Scr. Metall.*, 1990, **24**, 267–272.

9. TORABIAN, H., PATHAK, J. P. AND TIWARI, S. N. — Wear characteristics of Al–Si alloys, *Wear*, 1994, **172**, 49–58.

10. ALPAS, A. T. AND ZHANG, J. — Effect of SiC particulate reinforcement on the dry sliding wear of aluminium–silicon alloys (A356), *Wear*, 1992, **155**, 83–104.

11. ALPAS, A. T. AND ZHANG, J. — Wear rate transitions in cast aluminium–silicon alloys reinforced with SiC particles, *Scr. Metall.*, 1992, **26**, 505–509.

12. PRAMILA BAI, B. N. DWARAKADASA, E. S. AND BISWAS, S. K. — Scanning electron microscopy studies of wear in LM-13 and LM-13 graphite particulate composite, *Wear*, 1982, **76**, 211–220.

13. MODI, O. P., PRASAD, B. K., YEGNESWARAN, A. H. AND VAIDYA, M. L. — Dry sliding wear behaviour of squeeze-cast aluminium alloy-silicon carbide composites, *Mater. Sci. Engng A.*, 1992, **151**, 235–245.

14. SOMI REDDY, A., PRAMILA BAI, B. N., MURTHY, K. S. S. AND BISWAS, S. K. — Wear and seizure of binary Al–Si alloys, *Wear*, 1994, **171**, 115–127.

15. KABAYASHI, K. G. AND KAWAMOTO, M. — Influence of silicon content and grain size of primary silicon crystals on the wear of high silicon aluminium alloys, *Bull. Univ. Osaka Prefecture A*, 1968, **17**, 199–216.

16. STONEBROOK, E. E. — Aluminium alloy with high silicon content, *Mod. Cast.*, 1960, **38**, 111–114.

17. DEWHURST, E. V. — Gravity die casting of aluminium–silicon alloy on pistons, *Br. Foundryman*, 1966, **59**, 1–11.

18. VANDELLI, G. — The resistance to dry sliding wear of some cast heat resistant aluminium alloys, *Aluminio*, 1968, **37**, 121–129.

19. SARKAR, A. D. — Wear of aluminium-silicon alloys, *Wear*, 1975, **31**, 331–343.

20. CLEGG, A. J. AND DAS, A. A. — Wear of hypereutectic aluminium–silicon alloy, 1977, **43**, 367–373.

21. JALEEL, T. K. A., RAMAN, N., BISWAS, S. K. AND MURTHY, K. S. S. — Effect of structural modification and load on the wear of a hypereutectic aluminium–silicon alloy, *Aluminium*, 1984, **60**, E.787–E.789.

22. CLARKE, J. AND SARKAR, A. D. — Wear characteristics of as-cast binary aluminium–silicon alloys, *Wear*, 1979, **54**, 7–16.

23. SARKAR, A. D. AND CLARKE, J. — Friction and wear of aluminium–silicon alloys, *Wear*, 1980, **61**, 157–167.

24. ANDREWS, J. B., SENEVIRATNE, M. V., ZIER, K. P. AND JETT, T. R. — The influence of silicon content on the wear characteristics of hypereutectic Al–Si alloys, *ASME Int. Conf. on Wear of Materials*, 1985, pp. 180–186.

25. HANNA, H. A. AND SHEHATA, F. — Friction and wear of Al–Si alloys, *Lubric. Engng*, 1993, **49**, 473–476.

26. LONG, T. T., NISHIMURA, T., AISAKA, T. AND MORITA, M. — Wear resistance of Al–Si alloys and aluminium matrix composites, *Mater. Trans., J. Inst. Met.*, 1991, **32**, 185–188.

27. PRAMILA BAI, B. N. AND BISWAS, S. K. — Characterization of dry sliding wear of Al–Si alloys, *Wear*, 1987, **120**, 61–74.

28. PRAMILA BAI, B. N. AND BISWAS, S. K. — Effect of magnesium addition and heat treatment on mild wear of hypoeutectic aluminium–silicon alloys, *Acta Metall.*, 1991, **39**, 833–840.

29. RAZAVIZADEH, K. AND EYRE, T. S. — Oxidative wear of aluminium alloys, *Wear*, 1982, **79**, 325–333.

30. RAZAVIZADEH, K. AND EYRE, T. S. — Oxidative wear of aluminium alloys, Part II, *Wear*, 1983, **87**, 261–271.

31. PRAMILA BAI, B. N. AND BISWAS, S. K. — Mechanism of wear in dry sliding of a hypoeutectic aluminium alloy, *Lubric. Engng*, 1987, **43**, 57–61.

32. PRAMILA BAI, B. N. AND BISWAS, S. K. — Sub-surface deformation in dry sliding of hypoeutectic Al–Si alloys, *J. Mater. Sci.*, 1984, **19**, 3588–3592.